

AD-A153 939

AN EVALUATION AND PREPARATION OF FERROMAGNETIC LIQUID
COMPOSITES FOR USE A. (U) UNIVERSITY COLL OF NORTH
WALES BANGOR DEPT OF PHYSICS J POPPLEWELL ET AL.

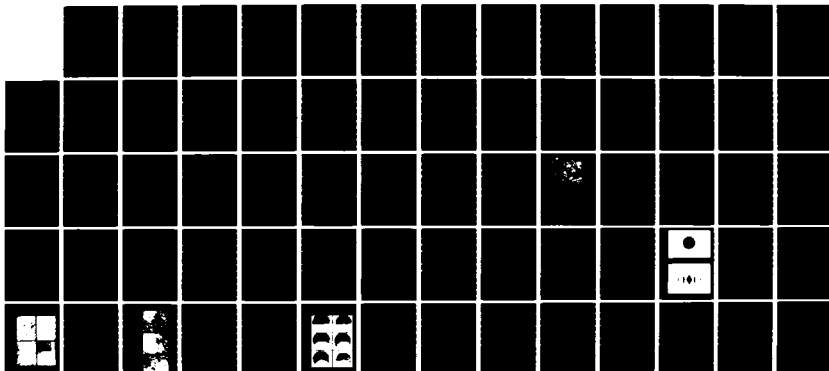
1/1

UNCLASSIFIED

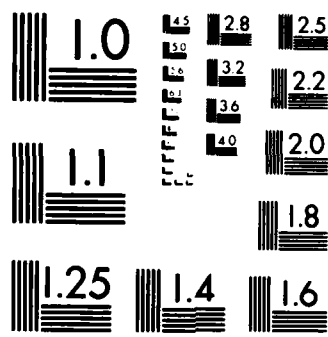
OCT 84 R/D-4130-R-M5 DAJA45-83-C-0026

F/G 20/3

NL



END



MICROCOPY RESOLUTION TEST CHART
NATIONAL BUREAU OF STANDARDS-1963-A

AD-A153 939

AN EVALUATION AND PREPARATION OF FERROMAGNETIC LIQUID COMPOSITES
FOR USE AT MILLIMETER WAVELENGTHS

First Annual Technical Report

by

DR J POPPLEWELL (PRINCIPAL INVESTIGATOR)

DR K O'GRADY

DR J P LLEWELLYN

MR P DAVIES

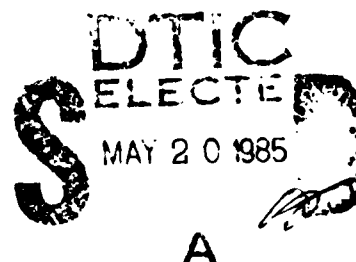
OCTOBER 1984

European Research Office
United States Army
London W 1 England

Contract Number DAJA 45-83-C-0026

Department of Physics
University College of North Wales
Bangor, Gwynedd, UK

Approved for public release; distribution unlimited



DTIC FILE COPY

UNCLASSIFIED

R&D 4130-R-MS

SECURITY CLASSIFICATION OF THIS PAGE (When Data Entered)

REPORT DOCUMENTATION PAGE		READ INSTRUCTIONS BEFORE COMPLETING FORM	
1. REPORT NUMBER R&D 4130-R-MS	2. GOVT ACCESSION NO. AD-7153	3. RECIPIENT'S CATALOG NUMBER 939	
4. TITLE (and Subtitle) An Evaluation of the Properties of Ferromagnetic Liquids at Millimeter Wavelengths		5. TYPE OF REPORT & PERIOD COVERED First Annual Technical Report Oct 83 - Oct 84	
		6. PERFORMING ORG. REPORT NUMBER	
7. AUTHOR(s) J. Popplewell, K. O'Grady, J. P. Llewellyn and P. Davies		8. CONTRACT OR GRANT NUMBER(s) DAJA45-83-C-0026	
9. PERFORMING ORGANIZATION NAME AND ADDRESS University College of North Wales Bangor, Gwynedd, UK		10. PROGRAM ELEMENT, PROJECT, TASK AREA & WORK UNIT NUMBERS 6.11.02A IT161102BH57-04	
11. CONTROLLING OFFICE NAME AND ADDRESS USARDSG-UK Box 65, FPO NY 09510		12. REPORT DATE Oct, 84	
		13. NUMBER OF PAGES 57	
14. MONITORING AGENCY NAME & ADDRESS (if different from Controlling Office)		15. SECURITY CLASS. (of this report) Unclassified	
		15a. DECLASSIFICATION DOWNGRADING SCHEDULE	
16. DISTRIBUTION STATEMENT (of this Report) Approved for Public Release; Distribution Unlimited			
17. DISTRIBUTION STATEMENT (of the abstract entered in Block 20, if different from Report)			
18. SUPPLEMENTARY NOTES			
19. KEY WORDS (Continue on reverse side if necessary and identify by block number) Ferrofluids, Composites, Thin Films, Magneto-Optics, Microwave, Magnetisation			
20. ABSTRACT (Continue on reverse side if necessary and identify by block number) Magnetic materials consisting of ferrofluids and ferrofluid composites i.e. mixtures of ferrofluid with metallic tin or non-metallic polystyrene or glass particles (0.2 μm to 25 μm diameter) have been prepared and studied. The samples in the form of thin films 1 to 10 μm thick have been examined using magnetic measurements and optical and microwave techniques. The measurements indicate that the films have (1) a magnetic anisotropy with a 30 % reduction in magnetisation with the plane of the film perpendicular to the field direction (2) a birefringence at both optical and microwave			

UNCLASSIFIED

SECURITY CLASSIFICATION OF THIS PAGE (When Data Entered)

UNCLASSIFIED

SECURITY CLASSIFICATION OF THIS PAGE(When Data Entered)

20.. Continued

frequencies. Particle conformations in the presence of a magnetic field have also been studied and related to theory, which gives the effective diamagnetic magnetic moment/ particle $\approx 10^{-9} - 10^{-10}$ emu.

Accession For	
NTIS GRA&I	<input checked="checked" type="checkbox"/>
DTIC TAB	<input type="checkbox"/>
Unannounced	<input type="checkbox"/>
Justification	
By	
Distribution/	
Availability Codes	
Dist	Avail and/or Special
AI	

UNCLASSIFIED

SECURITY CLASSIFICATION OF THIS PAGE(When Data Entered)

TABLE OF CONTENTS

<u>List of Symbols</u>	1
<u>Abstract</u>	2
<u>Introduction</u>	3
1. <u>Magnetic Properties of Ferrofluids</u>	5
(a) (i) Modes of Magnetisation in Ferrofluids	5
(ii) Energy of a Colloidal Particle in a Magnetic Field.	6
(iii) Effects of Dipolar Interactions (Curie-Weiss Behaviour)	7
(b) Composites Consisting of Polystyrene Spheres in Ferrofluids	8
(c) Labyrinthine Instability in Ferrofluids	10
(d) Optical Behaviour of Composite Colloids	10
2. <u>Experimental Procedure</u>	
(a) Preparation of Ferrofluids	13
(i) Preparation of Ferrofluids Containing Magnetite Particles	13
(ii) Preparation of Ferrofluids Containing Cobalt Particles	13
(b) Preparation of Composite Colloids	15
(i) Preparation of Optical Samples	15
(ii) Preparation of Microwave Samples	18
(c) Preparation of Labyrinthine Instability Plates.	18
(d) Magnetic Measurements	18
(e) Optical Birefringence Measurements.	20
(f) Diffraction Experiments	20
(g) Technique for Observing Labyrinthine Instability	23
(h) Microwave Experiments	23
3. <u>Results and Discussions</u>	28
(a) Physical Particle Size Analysis	28

(ii)

(b) Magnetic Measurements	31
(i) The magnetisation Curve and Particle Size	31
(ii) Superparamagnetic Behaviour of Ferrofluids	34
(iii) Curie-Weiss Behaviour and Chain Formation	34
(c) Thin Film and Concentration Measurements	38
(i) Thin Films of Ferrofluids and Composite Colloids	38
(ii) Measurement of Concentration of Spheres in a Ferrofluid	40
(d) Diffraction Measurements	43
(e) Micrographs of Composite Colloids	45
(f) Observation of Labyrinthine Instability	48
(g) Optical Birefringence Results.	48
(h) Microwave Results	50
4. <u>Conclusions and Recommendations</u>	52
5. <u>Acknowledgements</u>	54
6. <u>References</u>	55

LIST OF FIGURES

<u>Figure</u>	<u>Caption</u>
1.1	Composite Colloid
1.2	Idealised Labyrinthine Pattern
2.1	Reaction Mechanism for Producing Magnetite Particles
2.2	Surfactant Coating of Magnetite Particles
2.3	Apparatus Used for the Preparation of Ferrofluids
2.4	Composite Colloid Sample
2.5	Cell for Microwave Measurements
2.6	Cell for Observing Labyrinthine Instability Phenomena
2.7	Optical Birefringence Apparatus
2.8	Arrangement for Observing Diffraction Patterns
2.9	Aerial View of Labyrinthine Instability Experimental Arrangement
2.10	Fourier Transform Spectrometer
2.11	A typical Interferogram of Decalin Based Magnetite Fluid
3.1	Particle Size Distribution for a Ferrofluid Containing Fe_3O_4 Particles
3.2	Room Temperature (293 K) Magnetisation Curves for Cobalt Ferrofluids
3.3	Low and High Field Data
3.4	Magnetisation Curves in the Liquid Phase
3.5	χ_i and $1/\chi_i$ vs. Temperature for a Sample with $\bar{D}=121 \text{ \AA}$
3.6	χ_i and $1/\chi_i$ vs. Temperature for a Sample with $\bar{D}=46 \text{ \AA}$
3.7	Magnetisation Curves of Thin Film Colloids
3.8	Low Field Magnetisation Curves for Composite Colloid
3.9	Absorption vs. Wavenumber Curve
3.10	Cell Orientation for Microwave Experiments

SYMBOLS

τ	-	Relaxation time
K	-	Anisotropy constant
η	-	Viscosity
d	-	Particle diameter
D_s	-	Shliomis diameter
μ	-	Particle magnetic moment
H	-	Applied field
T_o	-	Ordering temperature
I	-	Magnetisation of the fluid emu/cc
I'	-	Magnetisation of the bulk emu/cc
I_s	-	Saturation magnetisation emu/cc
ϕ	-	Angle between μ and easy axis
θ	-	Angle between μ and H
χ	-	Magnetic susceptibility
a	-	Dipole/dipole separation
θ'	-	Angle between H and the plane of the film
λ	-	Wavelength
β	-	Diffraction angle

ABSTRACT

Keywords : Ferrofluids, Composites, Thin Films, Magneto-Optic, Microwave, Magnetisation.

Magnetic materials consisting of ferrofluids and ferrofluid composites i.e. mixtures of ferrofluid with metallic tin or non-metallic polystyrene or glass particles ($0.2\mu\text{m}$ to $25\mu\text{m}$ diameter) have been prepared and studied. The samples in the form of thin films 1 to $10\mu\text{m}$ thick have been examined using magnetic measurements and optical and microwave techniques. The measurements indicate that the films have (1) a magnetic anisotropy with a 30% reduction in magnetisation with the plane of the film perpendicular to the field direction (2) a birefringence at both optical and microwave frequencies. Particle conformations in the presence of a magnetic field have also been studied and related to theory, which gives the effective diamagnetic magnetic moment/particle $\approx 10^{-9}$ to 10^{-10} emu.

*... = 10 to 100 ...
...
...
...
...
...
...
...*

INTRODUCTION

The optical properties of magnetic fluids have been the subject of recent studies by Davies and Llewellyn (1979) (1980), Mehta (1983). Llewellyn (1983) has assumed a form or shape birefringence explains the experimental observation. Bradbury, Menear and Chantrell (1984) have considered theoretical interpretations based on Monte-Carlo calculations on weakly interacting particles. It is fair to comment, however, that the origin of such phenomena as the birefringence, dichroism and Faraday rotation is still not firmly established and there is currently much disagreement.

The purpose of this work is to investigate at microwave frequencies (1-4mm wavelengths) those magnetic fluids which show birefringence, dichroism and Faraday rotation at optical frequencies. The objective is to develop materials with significant effects which can then be studied in depth. Following this study will be an assessment of the applications of these materials in such devices as modulators, polarisers, isolators and high speed shutters.

Magnetic fluids containing Fe_3O_4 or cobalt particles have been prepared and studied using magnetisation measurements. These fluids can be characterised in this way prior to further investigation using optical techniques. This is necessary if the processes giving rise to optical and microwave properties are to be understood.

New novel composite materials reported by Skjeltorp (1983) show interesting features which are likely to lead to unusual properties in the optical and microwave regions. The latter possibility was brought to the attention of the investigators by Dr.F.Rothwarf of the European Research Office and an extensive study on this material has been made during the last year. Details are given in later sections of the Report. New materials containing powders in magnetic fluid have also been prepared and investigated.

It was intended that the bulk of the microwave study should be undertaken at the National Physical Laboratory, Teddington. Due to unforeseen circumstances relating to recent changes in agreements on collaboration and patent rights, work at the NPL will not now be possible. Dr.Jim Birch (NPL) is still agreeable to collaborate and will assist in developing a Fourier Transform Spectrometer at Bangor. Assistance in microwave studies

has also been provided by Dr.G.J.Evans (Chemistry Department U.C. Aberystwyth) and British Telecom, Ipswich who have made available a Grubb — Parsons F.T. Spectrometer for microwave studies. The current position is that most microwave studies will be undertaken at Bangor with assistance from Dr.Jim Birch.

1. MAGNETIC PROPERTIES OF FERROFLUIDS

Ferrofluids are colloidal dispersions of ferro or ferrimagnetic particles dispersed in a carrier liquid. Typical carrier liquids are water, diesters, hydrocarbon oils which may be polar or non-polar, silicone oils etc. The particulate materials used are usually the spinel ferrites or ferromagnetic elements or alloys. Particle sizes are in general 10 nm and the dispersion is maintained by the action of a surface active agent (surfactant). Hence a ferrofluid is a three component system which derives its magnetic behaviour solely from the fine magnetic particles in the dispersion. Accordingly the magnetic properties of ferrofluids are determined by the properties of the particles themselves which, because of their small size are invariably single domain.

1(a)(i) Modes of Magnetisation in Ferrofluids

Ferrofluids are unique magnetic systems since the particles in the colloid are free to move. Because of this fact two distinct modes of alignment of the magnetic moments with an applied field are possible. Firstly, the moments may align by bulk rotation of the particle itself with the magnetic moment locked in an 'easy' anisotropy direction; secondly, the moment may align by rotation over the anisotropy energy barrier via the well known process described by Néel (1947). The magnetisation of a ferrofluid proceeds by whichever mechanism has the shorter relaxation time, but in general both mechanisms contribute to the final value of the magnetisation due to the presence of a particle size distribution in the colloid.

The relaxation time for the Néel mechanism is given by

$$\tau_N^{-1} = f_0 \exp - (KV/kT) \quad 1.1$$

where f_0 is a constant ($f_0 = 10^{-9} \text{ s}^{-1}$), K is the effective anisotropy constant, V is the particle volume, k is Boltzmann's constant and T the absolute temperature, whereas the relaxation time for the bulk rotation mechanism is given by Shliomis (1974)

$$\tau_B = 6V\eta / kT \quad 1.2$$

where η = fluid viscosity. Equating 1.1 and 1.2 and setting $\eta = 1 \text{ cp}$ (typical for a ferrofluid) gives

$$D_S = \left\{ \frac{24kT}{\pi K} \right\}^{1/3} \quad 1.3$$

where D_s , the Shliomis Diameter, represents that particle size at which the transition from the Néel process to bulk rotation takes place.

Data given in Section 3(a) used with equations 1.1 and 1.2 enables the mode of magnetisation of the particles in a ferrofluid to be determined. The importance of this result is that optical effects reported in Section 3(g) may be related to the mode of magnetisation of the particles; that is it may determine whether or not optical and hence microwave anisotropy is observed. i.e. only ferrofluids containing large particles which rotate by the Brownian process give rise to a birefringence.

1. (a) (ii) Energy of a Colloidal Particle in a Magnetic Field

For a single domain particle of moment μ locked in a solid matrix the energy in an applied magnetic field H is given by

$$E = KV \sin^2 \phi - \mu H \cos \theta \quad 1.4$$

at $T=0$

where ϕ is the angle between the magnetic moment vector and the anisotropy easy axis and θ is the angle between the moment and the applied field.

Unless the first term in equation 1.4 is very much less than the second the presence of anisotropy will prevent the observation of true superparamagnetic behaviour as reported by Bean and Livingston (1959). However, for the case of a ferrofluid where the particles are free to move it is unnecessary to consider the anisotropy energy and the energy of a particle in a field is simply

$$E = -\mu H \cos \theta \quad 1.5$$

as for a paramagnetic ion, and true superparamagnetic behaviour is to be expected with the magnetisation being described by the Langevin function

$$L(\alpha) = \coth \alpha - 1/\alpha \quad 1.6$$

where $\alpha = \mu H/kT$. In practice a sum of Langevin functions is required due to the particle size distribution in the system.

In section 3(b)(iii) data is presented which shows that to a first approximation ferrofluids do exhibit true superparamagnetic behaviour.

1(a)(iii) Effects of Dipolar Interactions (Curie - Weiss Behaviour)

Since the particles in a ferrofluid each contain a single magnetic domain the particles behave as submicroscopic magnetic dipoles and accordingly interact with one another through dipolar interactions. For a simple system of two particles with moments $\underline{\mu}_1, \underline{\mu}_2$, separated by a distance r , the energy of interaction E_i , is given by

$$E_i = \frac{1}{r^3} \left\{ (\underline{\mu}_1 \cdot \underline{\mu}_2) - 3 (\underline{\mu}_1 \cdot \underline{\hat{r}}) (\underline{\mu}_2 \cdot \underline{\hat{r}}) \right\} \quad 1.7$$

For systems of more than two particles it is not possible to write an analytic expression for E_i and numerical techniques must be used to examine the effects of magnetostatic interactions. A theoretical analysis which has produced useful results on the effect of the magnetostatic interactions has been carried out using Monte-Carlo techniques by Chantrell et al (1980).

Due to the magnetostatic interaction energy, equation 1.5 is imprecise for samples where interaction effects are believed to be significant. For this situation equation 1.5 becomes

$$E = - \mu H \cos \theta + E_i \quad 1.8$$

where E_i can be either positive or negative depending on the particle size and concentration.

In a recent publication (O'Grady et al (1983)) it has been shown that ferrofluids exhibit Curie - Weiss type behaviour and the magnetisation in low fields can be represented by

$$\bar{I} = \frac{\mu H}{3k(T-T_0)} \quad 1.9$$

where \bar{I} is the reduced magnetisation I/I_s , I_s is the saturation moment of the sample. The temperature T_0 is an ordering temperature which represents that temperature at which the particles in the colloid take up ordered positions in the fluid and form chains of particles up to several microns long. This is an effect resulting from magnetostatic interactions and the use of equation 1.8 for the energy.

The Monte-Carlo simulation of Chantrell et al has been further extended by Menear et al (1983)(1984) who have been able to predict a magnetic ordering effect resulting in the formation of long chains of particles.

It is believed that the presence of such long chains may have a significant effect on the properties at optical and millimeter wavelengths and this phenomenon is therefore, of considerable interest to this project.

1(b) Composites Consisting of Polystyrene Spheres in Ferrofluids

A so called composite colloid of polystyrene spheres in a ferrofluid consists of monodispersed polystyrene spheres of typically one to fifty microns in diameter mixed in a ferrofluid. The remarkable properties of these colloids were first observed and reported by A.T.Skjeltorp (1983) of the Institute for Energy Technology in Kjeller, Norway who produced a composite colloid in the form of a thin film trapped between two glass plates and observed the behaviour of the spheres using an optical microscope. In a magnetic field the spheres possess an apparent magnetic moment due to the displacement of the superparamagnetic ferrofluid matrix. This apparent moment μ is given by

$$\mu = - \chi_{\text{eff}} V_{\text{ff}} H \quad 1.10$$

$$\text{Where } \chi_{\text{eff}} = \chi / \{ 1 - 4\pi\chi / 3 \} ,$$

V_{ff} is the displaced volume of fluid, χ is the volume susceptibility of the fluid and H the applied field parallel to the surface.

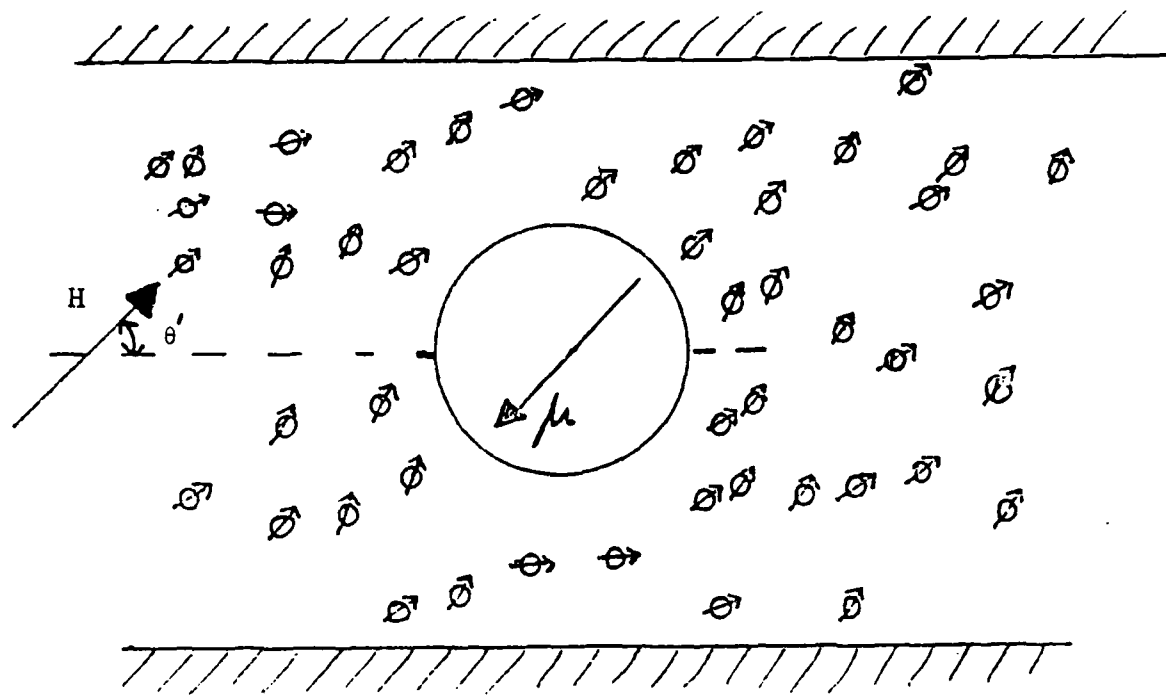
Skjeltorp reported the effects of dipolar interactions between the spheres as a function of the angle between the applied field H and the plane of the thin colloid. For fields parallel to the plane the interaction between the dipoles is attractive and they line up in long chains. For fields perpendicular to the plane the interaction is repulsive and the spheres take on the form of a two-dimensional hexagonal lattice. The interaction energy for two dipoles separated by a distance a , with a field at angle θ to the plane of the film is given (Figure 1.1) by

$$E = \mu^2 (1 - 3 \cos^2 \theta) / a^3 \quad 1.11$$

It was reported that the chains of the particles are observed to break up and the hexagonal arrays begin to form when $\theta = 70^\circ$. Similarly, the two-dimensional hexagonal structure is observed to 'melt' when

$$r = \frac{\text{dipole energy}}{\text{thermal energy}} = \frac{\mu^2 / a^3}{kT} < 60 \quad 1.12$$

Experimental observations regarding these phenomena are described and then discussed in Section 3(d).



ϕ Magnetic Moments of Fluid Particles

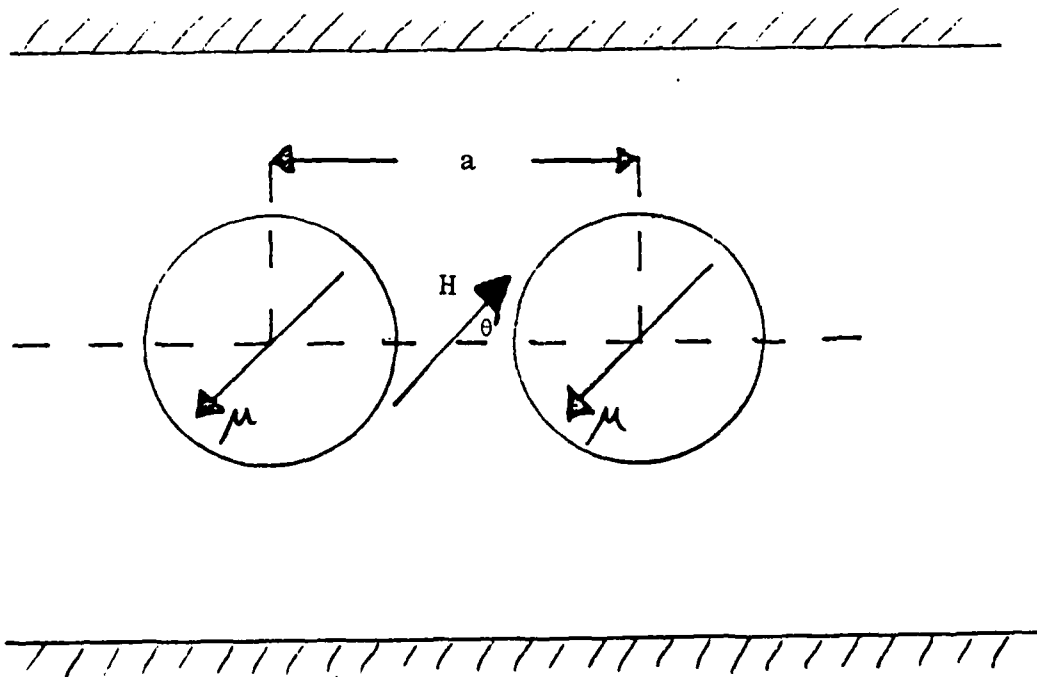


Fig. 1.1 Composite Colloid (i) One isolated sphere in ferrofluid.
(ii) Two interacting spheres.

1(c) Labyrinthine Instability in Ferrofluids

Another field dependent phenomenon concerning magnetic fluids is that of the labyrinthine instability. The instability characterised by a finger-like distortion of the surface of a ferrofluid was studied in order to investigate the possibility of controlling the finger growth with a magnetic field. The effect on optical and microwave properties produced by a well defined and uniform pattern was to be investigated provided the results of a preliminary investigation appeared promising. The results of this investigation are given in Section 3(e). A more general discussion of the background to the labyrinthine instability now follows.

When a ferrofluid is confined with an immiscible liquid between closely spaced parallel plates, and a uniform magnetic field is applied perpendicular to the plates a finger pattern is established due to an interfacial instability between the fluids (Tsebers (1980)). At critical intensities of the magnetic field, fingers of ferrofluid invade the non-magnetic immiscible liquid. Similarly the immiscible non-magnetic component invades the ferrofluid.

The final state of the process is the formation of a labyrinth pattern, photographs of which are shown in section 3(e).

The theory put forward by Rosensweig (1983) is a simplified one, which idealizes the labyrinth as a repeating pattern of parallel paths i.e. the presence of convolutions of the actual pattern is ignored. The idealized pattern is illustrated in Figure 1.2. The total energy of one period of the repeating pattern is calculated as the sum of the magnetostatic energy U_m and the interfacial energy U_s . A minimisation of energy can then be used to determine equilibrium spacing, since it is assumed that the instability is related to the tendency to reduce the energy of the demagnetizing field. For this preliminary study a detailed theoretical analysis is not necessary but can be found by consulting Romankiw et al (1975) and Rosensweig (1983).

1(d) Optical Behaviour of Composite Colloids

Since typical diffraction gratings have grating spacings in the range 80 to 600 lines per millimeter interesting diffraction effects would be expected from a monolayer of monodispersed polystyrene spheres in a ferrofluid.

As noted in Section 1(b) with no field applied the spheres are randomly arranged. Therefore, employing Babinet's principle the spheres will be expected to act as a single circular

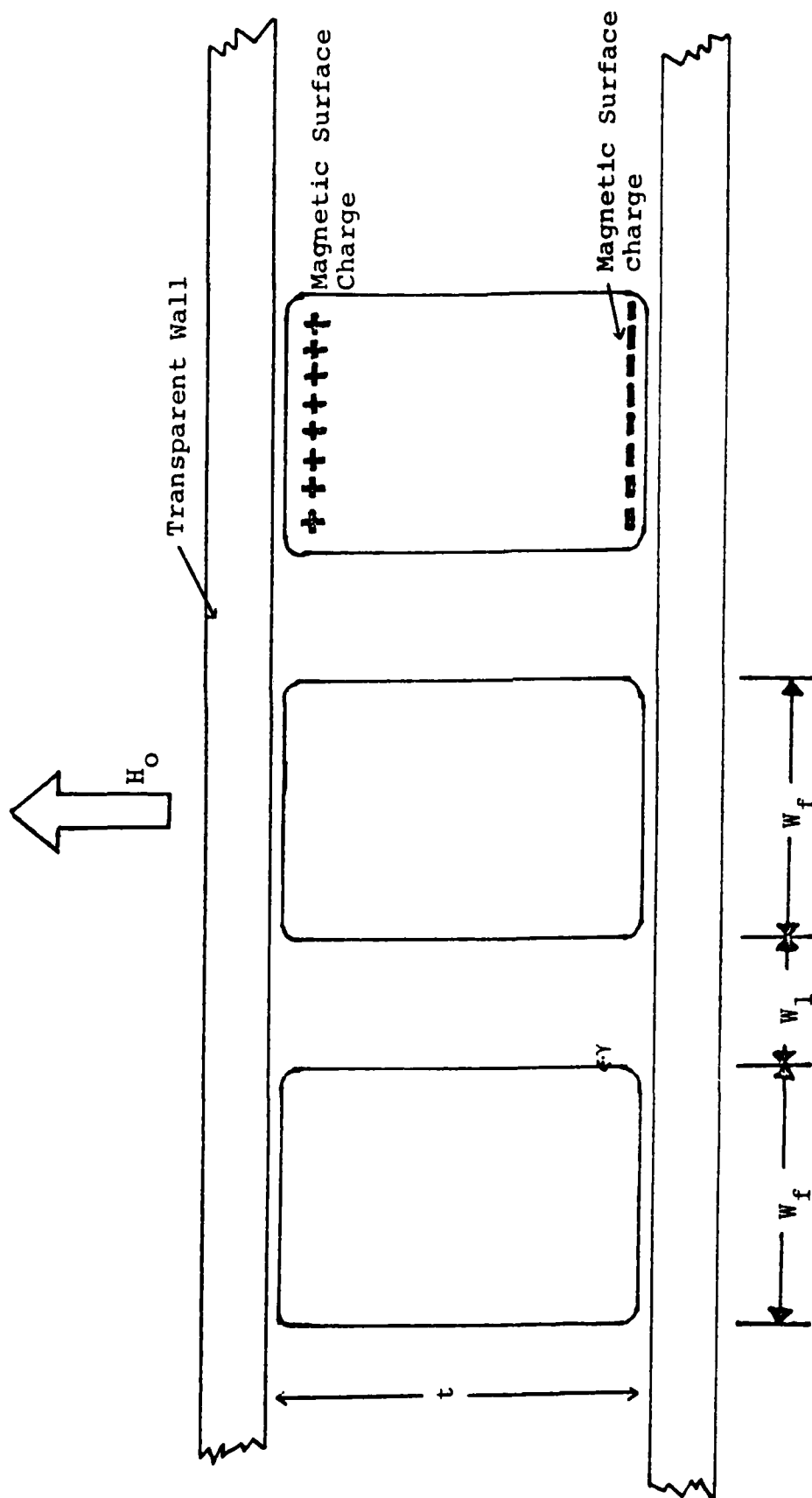


Fig. 1.2. Idealized Labyrinthine Pattern

diffracting aperture of diameter d , where d is the diameter of a single sphere. The angular radius of the first dark band of the resulting diffraction pattern is then given by the first zero of the Bessel function of the irradiance distribution; that is

$$\sin \beta = \frac{1.22\lambda}{d} \approx \beta \text{ (for small } \beta \text{)} \quad 1.13$$

Here λ is the wavelength of the light used. Since $\sin \beta$ is small, to a first approximation it can be equated to the distance from the centre of the diffraction pattern to the first dark band, h , divided by the focal length of the lens used to focus the diffraction pattern on the screen, f . i.e.

$$\sin \beta \approx \beta \approx \frac{h}{f} \text{ (for small } \beta \text{)} \quad 1.14$$

With a field applied parallel to the sample, i.e. perpendicular to the light path, the spheres will chain (see Section 1(b)). Taking a single chain of spheres and again employing Babinet's principle it can be seen that the chain will act as a $1 \times n$ diffraction grating, where n is the number of spheres in a chain. To a good approximation the spheres can be assumed to be touching and therefore the aperture spacing is equal to d . Again using diffraction theory and the distance between principal maxima in the diffraction pattern, d can be calculated.

Although these effects are unlikely to show any significant effects in the microwave region some interesting effects would be expected when the polystyrene spheres are replaced by conducting spheres. Some such composite materials have been prepared and are discussed in Section 3(d)

2.

EXPERIMENTAL PROCEDURE

2(a) Preparation of Ferrofluids

2(a)(i) Preparation of Ferrofluids Containing Magnetite Particles

The method used for producing surfactant coated magnetite was based on that given by Shimoiizaka et al (1980). Sodium oleate coated particles of magnetite (Fe_3O_4), approximately 100 Å in diameter were prepared in the following way.

A mixture of 130g of ferric chloride and 77g of ferrous sulphate (molar ratio 2:1) was dissolved in distilled water (Figure 2.1). The resulting solution was highly acidic (pH 2) and approximately 400 ml of 10M sodium hydroxide solution was added until the pH of the mixture had risen to a value of about 11. The solution was stirred for an hour at room temperature to form the Fe_3O_4 precipitate. An excess amount (21 ml) of oleic acid ($\text{CH}_3(\text{CH}_2)_7\text{C}-\text{C}(\text{CH}_2)_7\text{C}\overset{\text{O}}{\underset{\text{OH}}{\parallel}}$) was added to the mixture. Oleic acid is insoluble in water at pH7, but in alkali solution the acid dissociates due to the presence of sodium ions. The oleate ion is then free in solution. The oleate ions are chemisorbed onto Fe^{2+} ions at the surface of the magnetic particles and since there is an excess present, complete coating of each particle is ensured. Physisorption between sodium oleate molecules also occurs and forms a partial second layer over the magnetite (Figure 2.2)

Nitric acid was added until the pH was approximately 4.5 and the mixture was heated to 100°C. This coagulates the magnetite by converting the oleate ion in the second layer to hydrophobic free acid molecules. The coagulate was separated and repeatedly washed in acetone and distilled water to produce magnetite coated with a monolayer of oleate. The magnetite was then dried under vacuum and finally dispersed in an appropriate carrier.

Four liquids have been used as carriers. Isopar M, hexadecene, toluene and Decalin. The method of dispersion used was as follows. 5ml of the required carrier liquid was placed in a small beaker. The carrier was then gently heated and about 0.25g of oleic coated magnetite was added. The magnetite was then dispersed by continual stirring. By varying the amount of magnetite dispersed in a sample the magnetic strength of the resulting fluid could be varied. To ensure that the fluids did not contain large agglomerates which could have led to colloidal instability they were finally centrifuged at 3500 r.p.m. for 30 minutes. The top 75% of the resulting colloid was then decanted off and the residue discarded. In this manner a variety of ferrofluids were produced.

2(a)(ii) Preparation of Ferrofluids Containing Cobalt Particles

Ferrofluids containing cobalt particles were produced by decomposition of dicobalt octacarbonyl according to the method

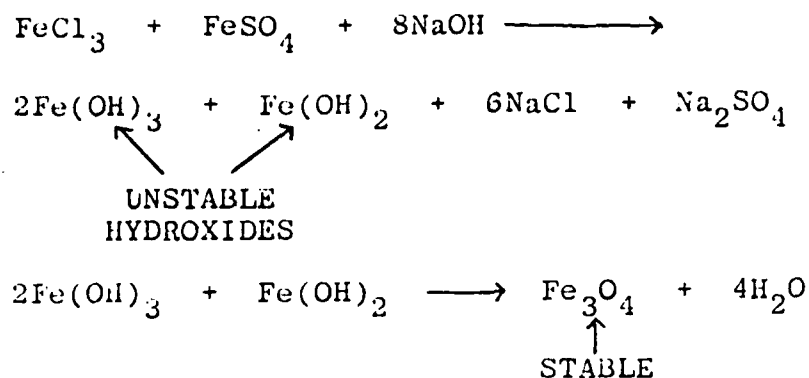


Fig.2.1 Reaction Mechanism for Producing Magnetite Particles

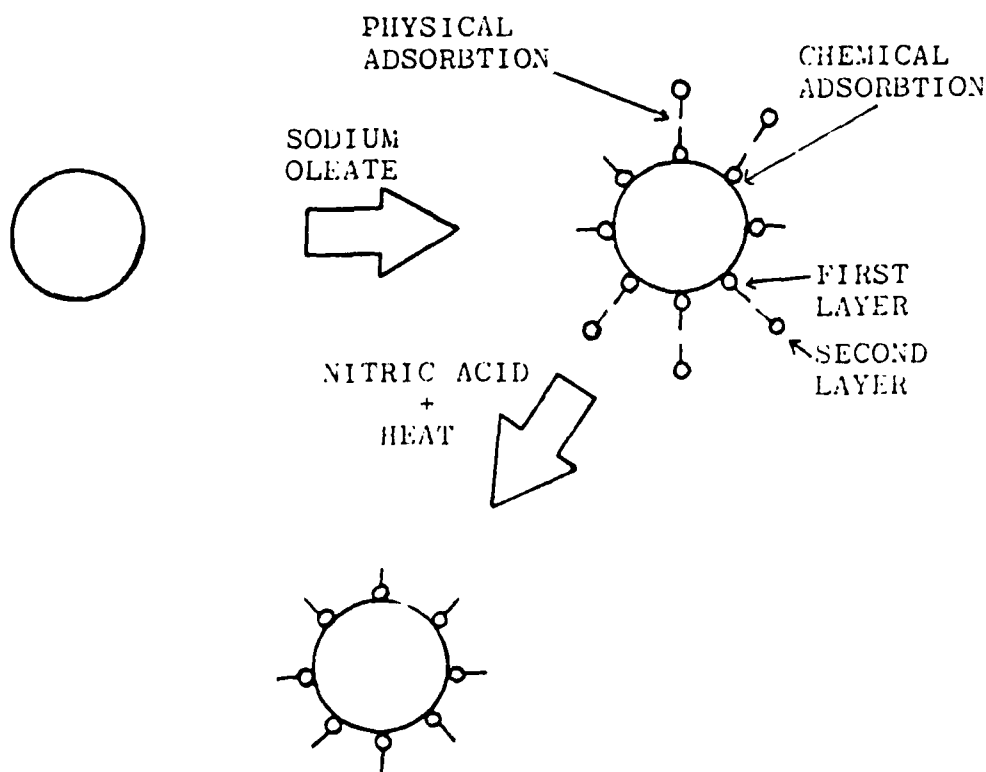


Fig.2.2 Surfactant Coating of Magnetite Particles

of Hess and Parker (1966). The reaction is carried out in a solution of surfactant which controls the size of the particles produced and forms a stable colloid similar to the magnetite fluids previously described.

The basic reaction is $\text{Co}_2(\text{CO})_8 \xrightarrow{\text{heat}} 2\text{Co} + 8(\text{CO})$

The apparatus used is shown in Figure 2.3. From the reaction it can be seen that each gram of carbonyl should produce 0.345g of cobalt metal. However, in practice only a 60% yield was achieved. The amount of surfactant used in these preparations was calculated as 40% by weight of the theoretical yield of cobalt metal. Thus to prepare 15ml of ferrofluid ($M_s = 300$ Gauss approx.), 1.4g of surfactant (e.g. oleic acid) was dissolved in 13.6 ml of toluene. An isomantle heater was then pre-heated to about 130°C. To the surfactant solution was added 10g of dicobalt octacarbonyl which was then placed in a three necked round-bottomed flask, fitted with a stirrer and a stuffing-gland seal. The apparatus was then assembled as in Figure 2.3 and the mixture stirred without heating for 10 minutes. The mantle was then raised and the solution heated rapidly. The solution was refluxed until the evolution of carbon monoxide ceased and then left to cool to room temperature with continual stirring. The resulting product was a black stable magnetic colloid of elemental cobalt particles. Ferrofluids in other hydrocarbon carriers can be prepared by mixing the original toluene based colloid with the desired carrier liquid and allowing the toluene to evaporate.

For a review of the many techniques for the preparation of ferrofluids see Charles and Popplewell (1980).

2(b) Preparation of Composite Colloids

2(b)(i) Preparation of Optical Samples

The composite colloid samples were made using the simple but effective method given by Skjeltorp, (1983). A typical sample containing 10.0µm polystyrene spheres and a 350 Gauss Isopar M based magnetite fluid (prepared according to the procedure given in section 2(a)) was made as follows. A few drops of water containing the polystyrene spheres in suspension were placed on a microscope slide and allowed to dry out. One drop of ferrofluid was then pipetted onto the slide and a glass cover slip placed on top (Figure 2.4). The cover slip was pressed down to squeeze out any excess ferrofluid. It was also necessary to move the cover slip in a circular motion while pressing down, in order to dislodge any spheres which might have become attached to the microscope slide. The sample was then sealed using an epoxy resin to prevent drying out. This was not completely successful since

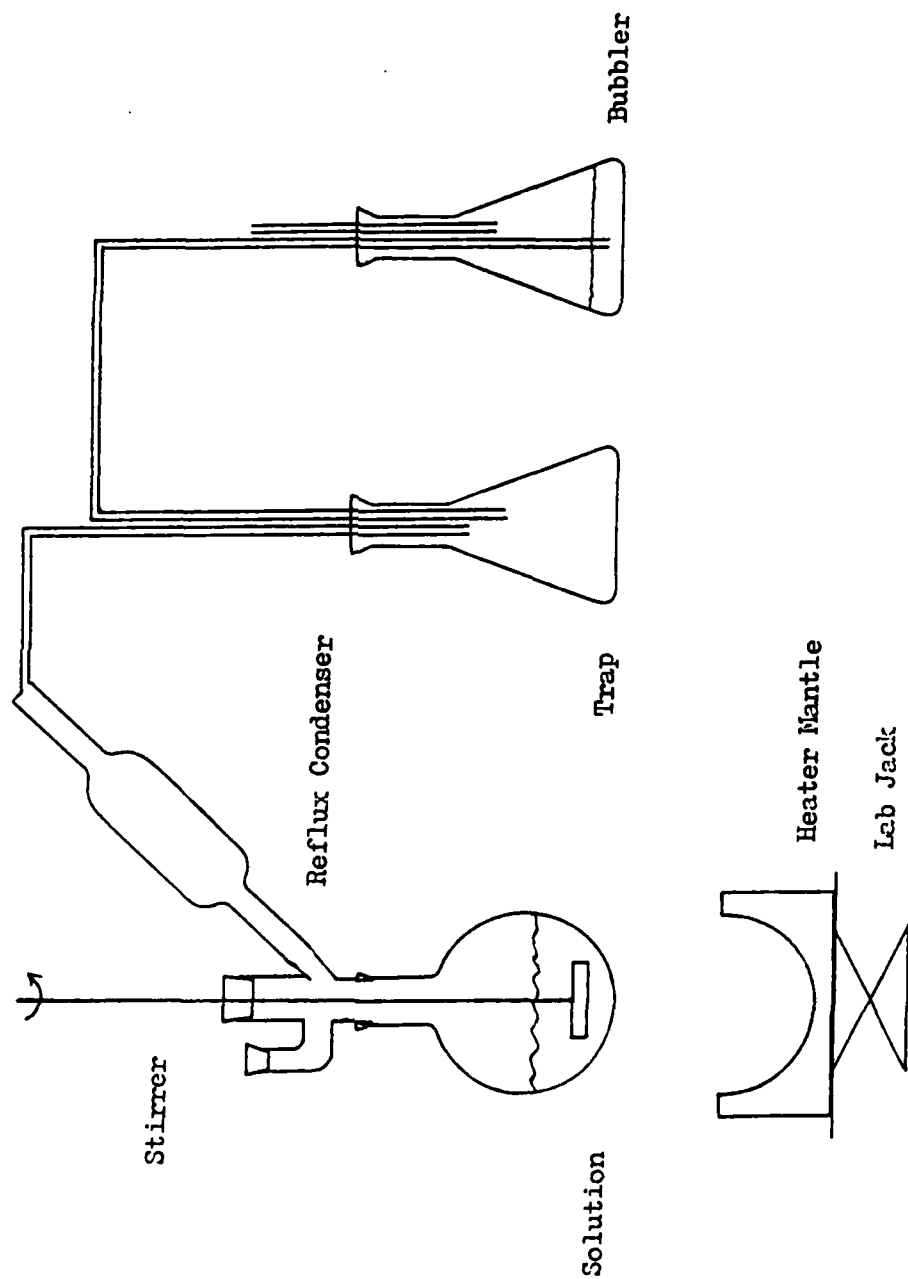


Fig. 2.3 Apparatus Used for the Preparation of Ferrofluids by the Carbonyl Process

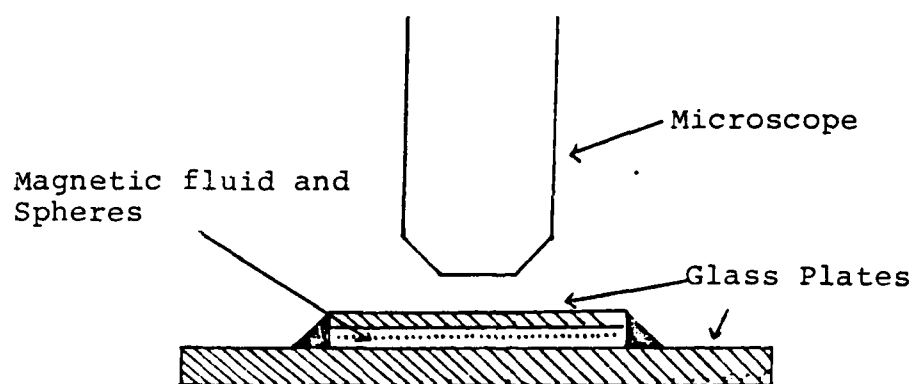


Fig.2.4 Composite Colloid Sample

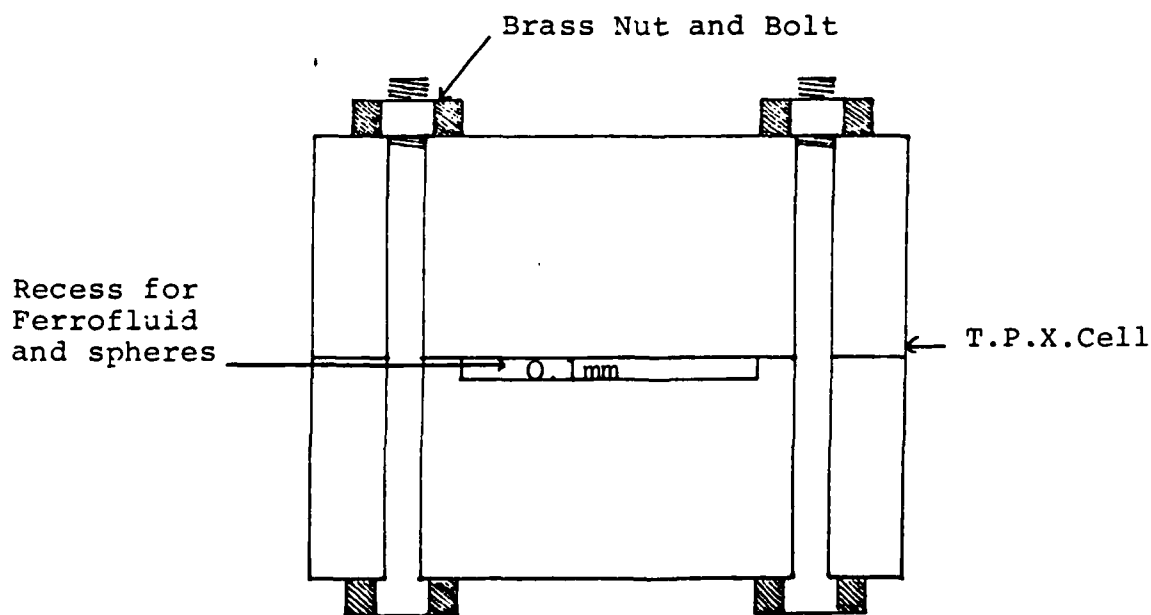


Fig.2.5 Cell for Microwave Measurements

over a period of weeks the samples dried out. Therefore, hexadecene, a carrier of lower vapour pressure than Isopar M, was used in producing subsequent samples.

2(b)(ii) Preparation of Microwave Samples

Glass could not be used in the preparation of microwave samples because of the high absorption at microwave frequencies. Therefore, a cell was designed and built (Figure 2.5) from T.P.X., a material which readily transmits in the wavelength range above 200 μ m. The spheres and ferrofluid were placed in the recess (path length 0.1 mm) and the cover bolted down to seal the sample.

Z-cut crystalline quartz plates which have a very high transmission at millimeter wavelengths were also used.

2(c) Preparation of Labyrinthine Instability Plates

The samples used for the investigation of labyrinthine instability were made up using glass plates and an epoxy resin as sealant. A square former, approximately 0.8mm thick, was placed between two glass plates, 70mm square. The plates were clamped in position and three sides were sealed with epoxy resin to form an open-ended cell of dimensions 70mm x 70mm x 0.8mm. The resin was allowed to set for about one hour after which the former was removed. Ferrofluid was then introduced into the cell using a syringe until it was half full. The upper half of the cell was then filled with distilled water containing 100 parts per million of surfactant (ethomeen C/25) to provide preferential wetting of the glass cell. The cell was then sealed with resin to prevent evaporation (Figure 2.6). The cell was placed between two electromagnet coils (Figure 2.10) with the pole pieces removed to enable photographs to be taken.

2(d) Magnetic Measurements

All the magnetic measurements described in this report were made using a Princeton Applied Research (PAR) 155 vibrating sample magnetometer with a resolution of 10^{-5} emu. The magnetometer was mounted on a conventional water cooled electromagnet capable of supplying fields of up to 10k Oe. The magnetic field was measured using a Bell-Gauss B-H 700 Hall Probe with a maximum resolution of 0.03 Oe calibrated using a proton magnetometer and standard magnets.

The magnetometer was fitted with an Oxford Instruments CF 1200 gas flow cryostat which enabled temperature variation

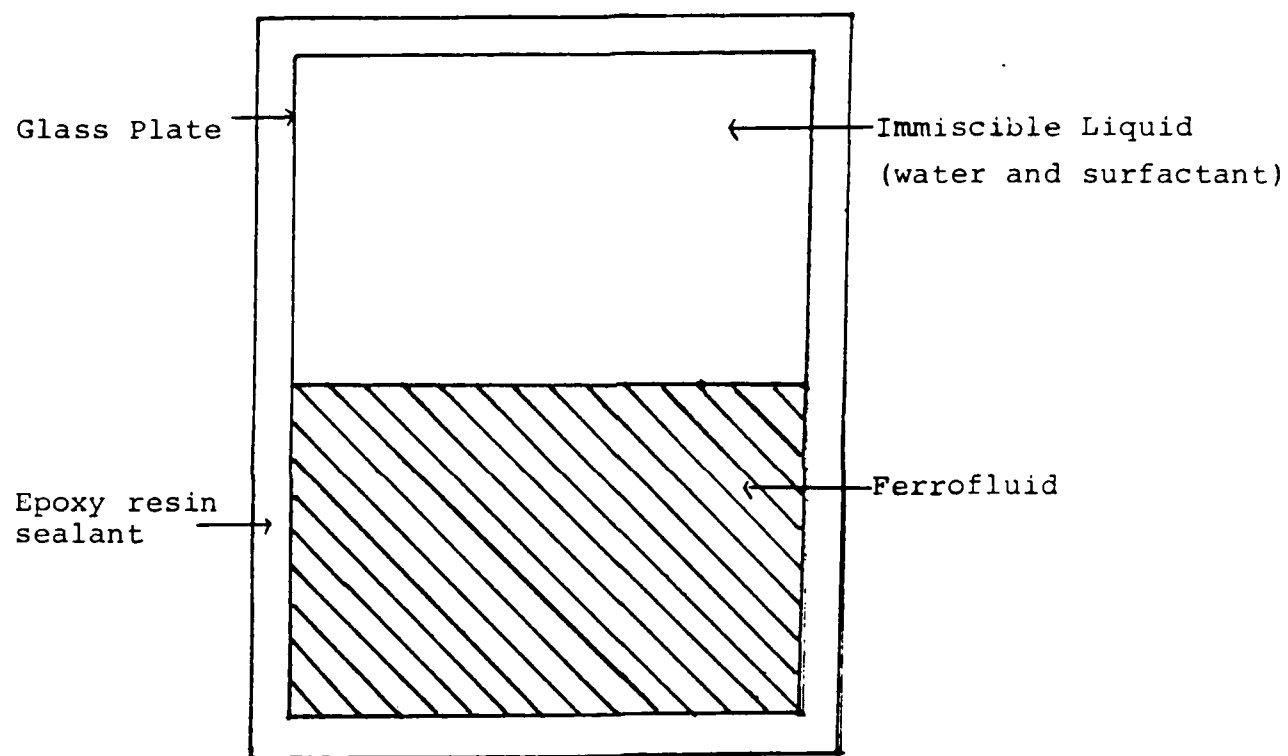


Fig. 2.6 Cell for observing labyrinthine instability phenomena

from 4K up to room temperature.

Each day before use the magnetometer was calibrated with a nickel sample and Hall probe zeroed. Because of the design of the vibrating assembly, measurements could be made as a function of angular rotation of the sample relative to the field direction without altering the resolution of the instrument. These measurements are of considerable importance in examining anisotropy in both ferrofluids and composite colloids.

2. (e) Optical Birefringence Measurements

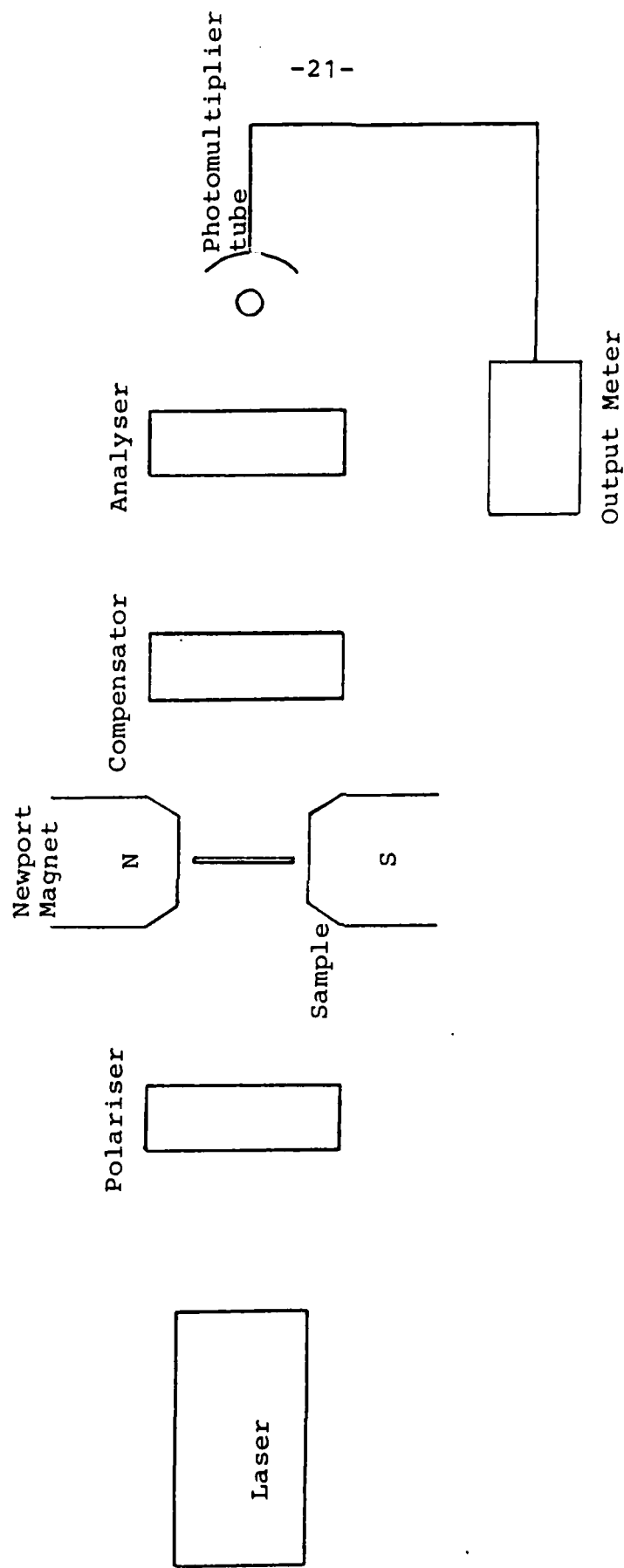
A brief study was made to observe any birefringence that might be induced in a sample containing a monolayer of polystyrene spheres in a ferrofluid. The experimental apparatus used is shown in schematic form in Figure 2.7. The light from the laser was polarised and passed through the sample, to which a magnetic field could be applied.

With the sample in position and zero applied field the compensator was adjusted to give a null reading on the output meter. A field was then applied to the sample. If birefringence occurred then the reading of the output meter was no longer zero. To measure the amount of birefringence the compensator was adjusted to give again a null. The birefringence of the sample is simply proportional to the change in the reading on the micrometer dial of the compensator. The analyser is used in dichroism experiments and was therefore not necessary in this study.

Three samples were investigated containing 10.0 μ m, 1.7 μ m and 0.22 μ m spheres in a hydrocarbon based ferrofluid with a saturation magnetisation of 400 Gauss.

2 (f) Diffraction Experiments

The experimental arrangement used to study the diffraction patterns of the composite colloids is shown in Figure 2.8. A Helium-Neon laser ($\lambda = 632.8\text{nm}$) was used to provide a coherent source of radiation. The laser beam was brought to a sharp focus using a short focal length lens. A pinhole was placed at the focal point of the lens to remove unwanted higher spatial frequencies present in the beam. The beam was then collimated and passed through the sample to be studied. The diffraction pattern produced by the sample was focussed onto a screen; for recording purposes a camera fitted with a 50mm focal length lens replaced the lens and screen. A magnetic field was applied to the sample using a Newport magnet and power supply.



-21-

Fig.2.7 Optical birefringence apparatus

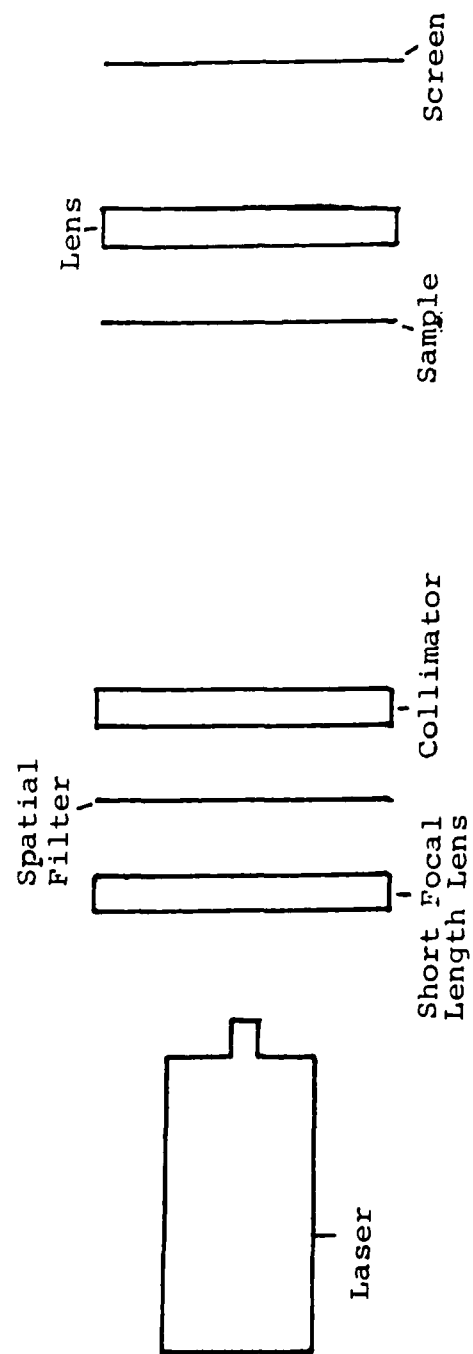


Fig. 2.8 Arrangement for Observing Diffraction Patterns

2 (g) Techniques for Observing Labyrinthine Instability

The experimental arrangement used in observing labyrinthine instability at the interface between a ferrofluid and an immiscible liquid is shown in Figures 2.9 (a) and 2.9 (b).

In order to produce uniform d.c. fields up to about 325 oersteds a large air cooled electromagnet was used with its pole pieces removed from the yoke. This arrangement enabled light to be shone through the plate under observation co-directional to the magnetic field, which was perpendicular to the plate. In order that the value of the field applied should be accurately known, the field current characteristic of the magnet was measured using a Bell Gauss 700 Hall probe, which was then removed to avoid obstructing the optical path. The whole experimental arrangement was mounted with the magnetic field horizontal and the plane of the plate lying in the vertical direction. This experimental arrangement suffered from the disadvantage that gravitational effects on the two liquids which had different densities, resulted in settling of the denser species. This facet of the experimental set-up is believed to have produced only minimal effects in the observed labyrinthine pattern.

Using the above arrangement various fields could be applied to a sample, and the labyrinthine pattern recorded by the camera.

2(h) Microwave Experiments

The Fourier Transform Spectrometer used in the microwave study is shown schematically in Figure 2.10. It is clearly desirable to choose a spectroscopic system giving an optimum transfer of energy from the source to the detector. Such a system uses a two-beam Michelson interferometer which has the highest throughput of any spectroscopic system. This is because it records all parts of the spectrum simultaneously (the so called multiplex advantage).

The interferometer was connected to a microcomputer which selected the component frequencies from the interference record observed by the detector, as the path difference between the two partial beams of the interferometer, Δ , was varied. A Fourier transform of the data from the detector provided an absorption versus wavelength plot, which could be recorded on a chart recorder as an interferogram, an example of which is shown in Figure 2.11. For further information regarding Fourier Transform Spectroscopy techniques see Chamberlain (1979) and Evans et al (1976).

The ferrofluids used in the microwave experiments had to be chosen carefully. The first series of experiments were unsuccessful since the carrier used was the same as that for the optical observations i.e. hexadecene. Hexadecene and Isopar M are very highly absorbing in the microwave range and could not, therefore, be used for these measurements. However toluene and

decalin ($C_{10}H_{18}$) trasmit at these wavelengths. Decalin was found to be more suitable since toluene has a very high vapour pressure and had a tendency to evaporate.

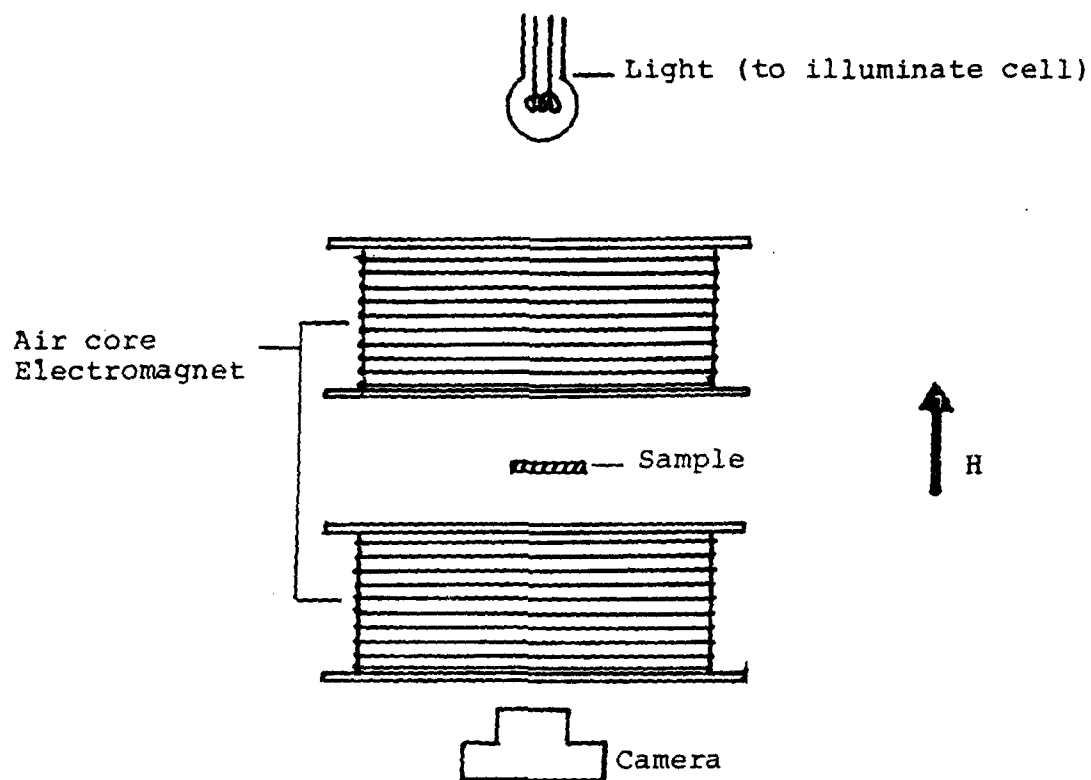


Fig. 2.9 (a) Aerial view of labyrinthine instability experimental arrangement

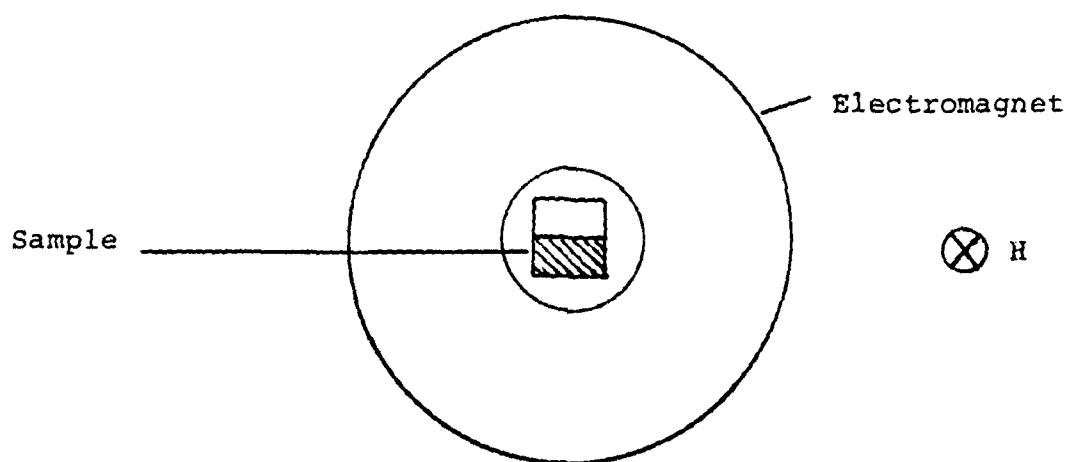


Fig. 2.9 (b) Side view.

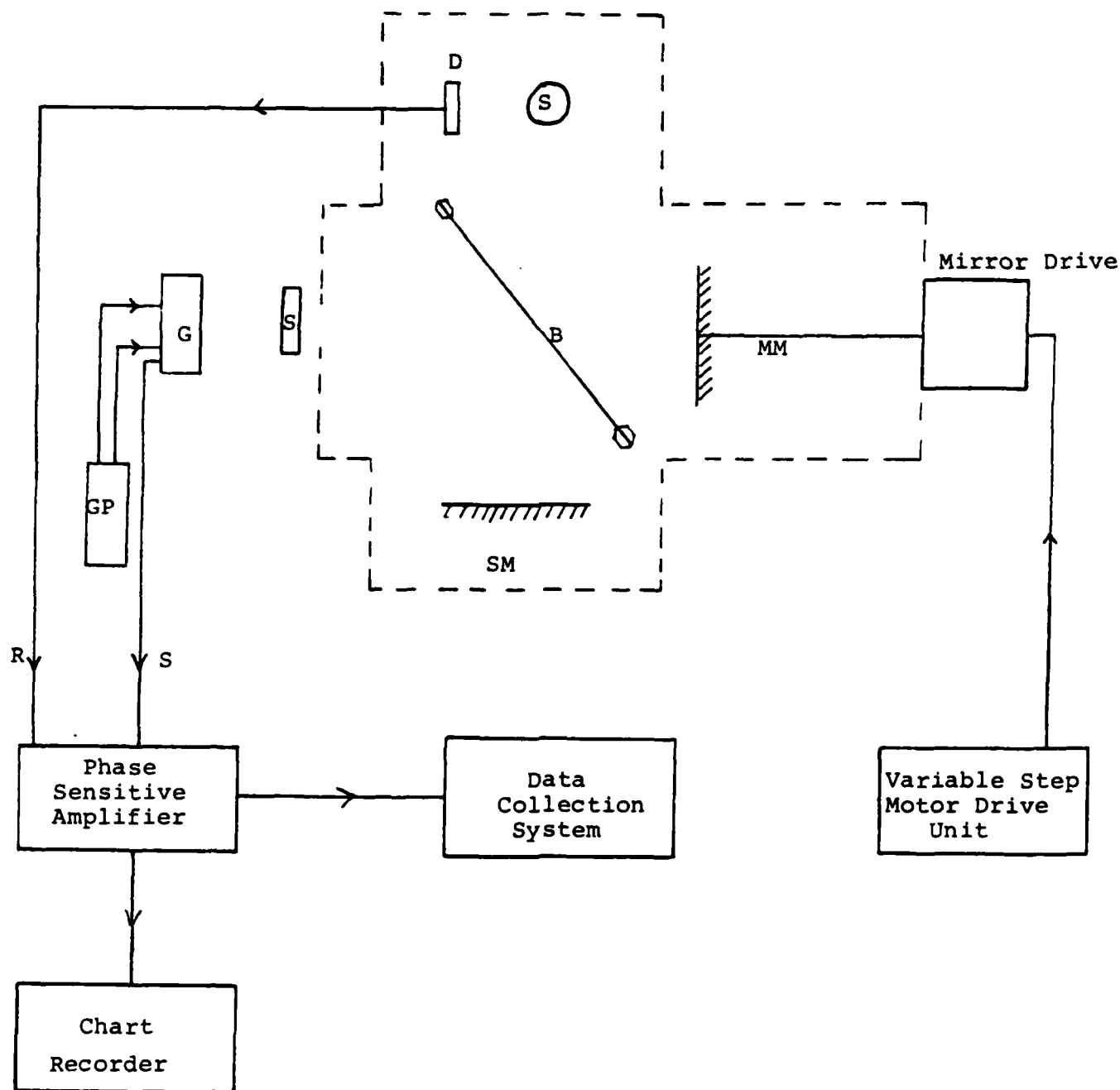


Fig. 2.10 Fourier Transform Spectrometer

Key: D, diode, S, source, MM, movable mirror, SM, stationary mirror, B, beam divider, G, detector, GP, detector power supply, R, reference, S, signal.

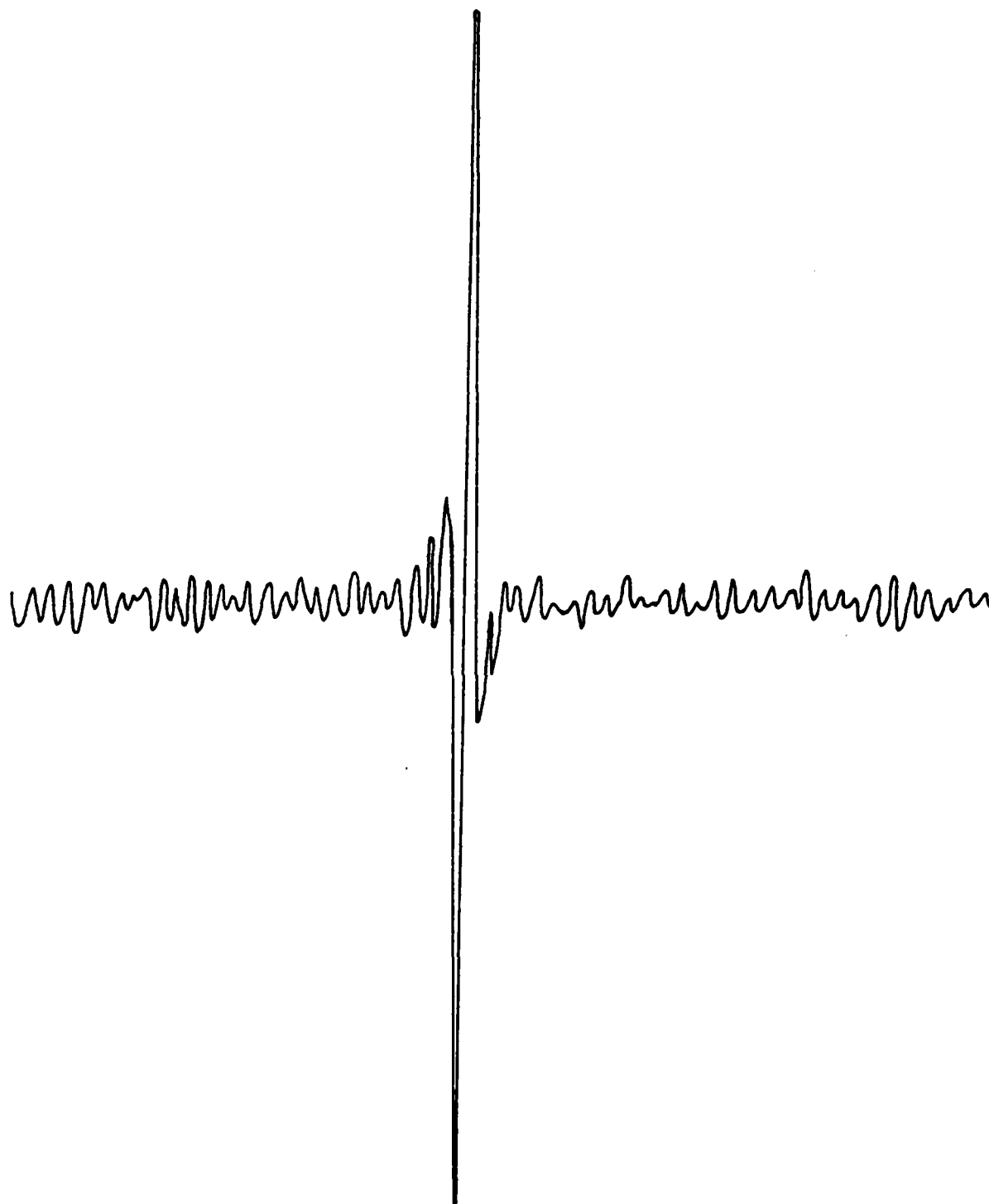


Fig. 2.11 A typical interferogram of
Decalin based Magnetite Fluid.

3.

RESULTS AND DISCUSSION

Before analysing the different materials prepared using ferrofluids, the ferrofluid itself was analysed by various techniques. Since the ferrofluid forms the basis for all the materials studied it is important that the ferrofluid is chosen to ensure maximum effect. Characterisation is undertaken by electron microscopy and magnetic measurements as indicated in the following sections.

3 (a) Physical Particle Size Analysis

Plate 1 shows two typical electron micrographs of magnetite particles and cobalt particles, obtained from samples of the ferrofluids used in the preparation of the composites. The particles were examined using an A.E.I. Corinth 275 electron microscope with a linear resolution of $<10\text{\AA}$. The micrographs all had a magnification between 250,000 and 300,000. The diameters of at least 500 particles on each micrograph were measured using the Zeiss particle size analyser. According to O'Grady and Bradbury (1983) particles prepared by chemical methods (e.g. decomposition of cobalt carbonyl or Shimoiizaka's "wet" method (section 2a)) have a Gaussian distribution of diameters. Figure 3.1 bears out this result; it shows the experimental fit of the particle diameters to a Gaussian distribution (solid line).

The mean of the diameters, \bar{D} and the standard deviation of the mean, σ were computed using O'Grady and Bradbury's particle size analysis software. The results are shown in the following table, together with magnetic size data (section 3(b) (i))

Particles	Physical Size		Magnetic Size	
	\bar{D} (\AA)	σ	D_{vm} (\AA)	σ_m
Fe_3O_4	98	0.19	82	0.22
Co	46	0.31	36	0.33
	121	0.20	108	0.23

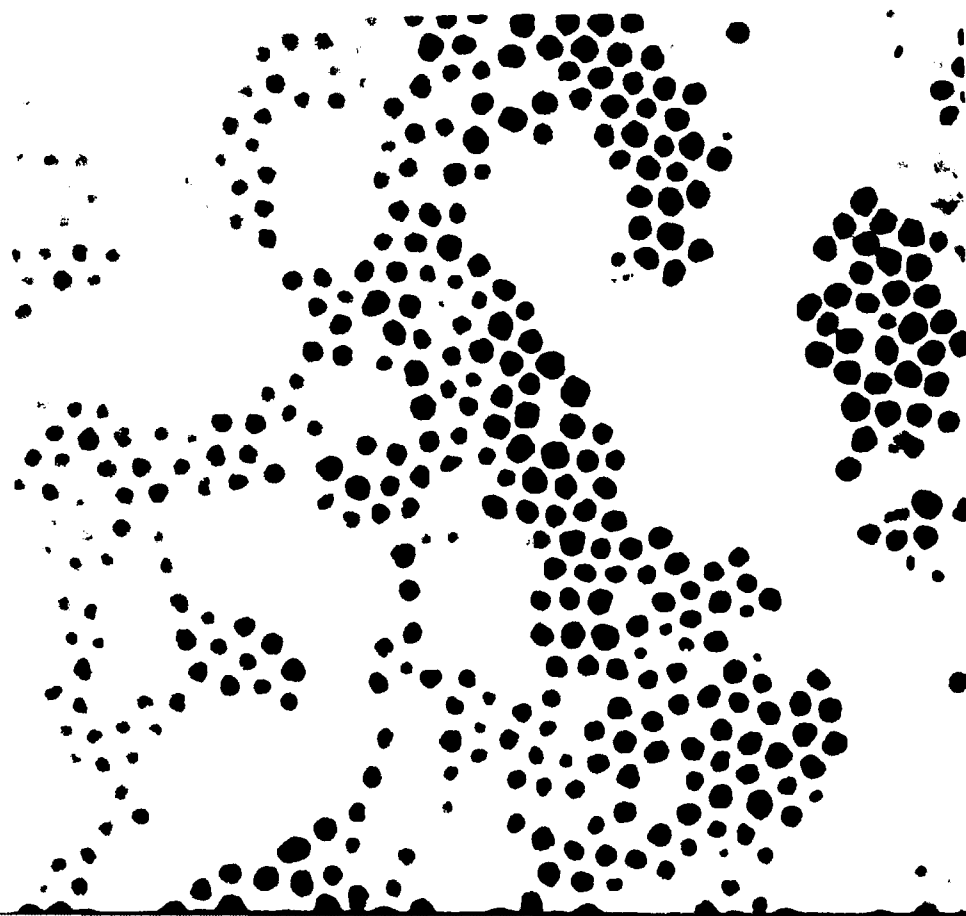
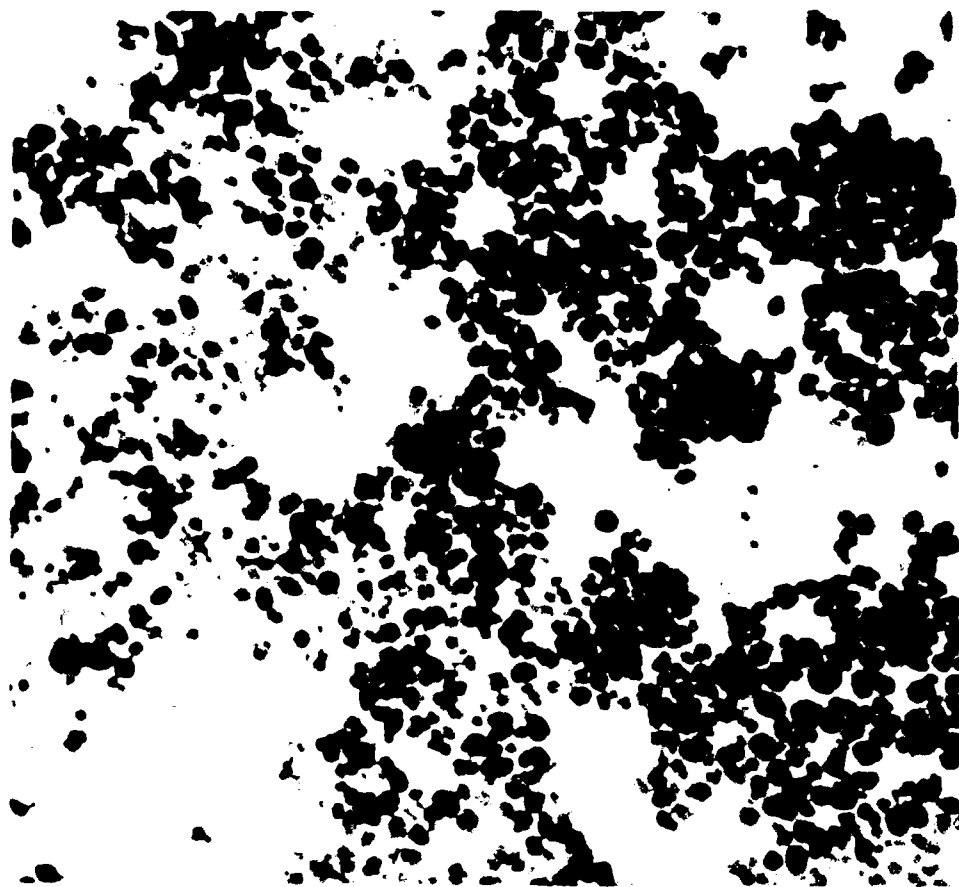
Table. 3.1. Typical Particle Size Data.

A more comprehensive mathematical discussion of particle size analysis is given in O'Grady and Bradbury (1983).

Plate 1. Ferrofluid Particles

Top: Magnetite

Bottom : Cobalt



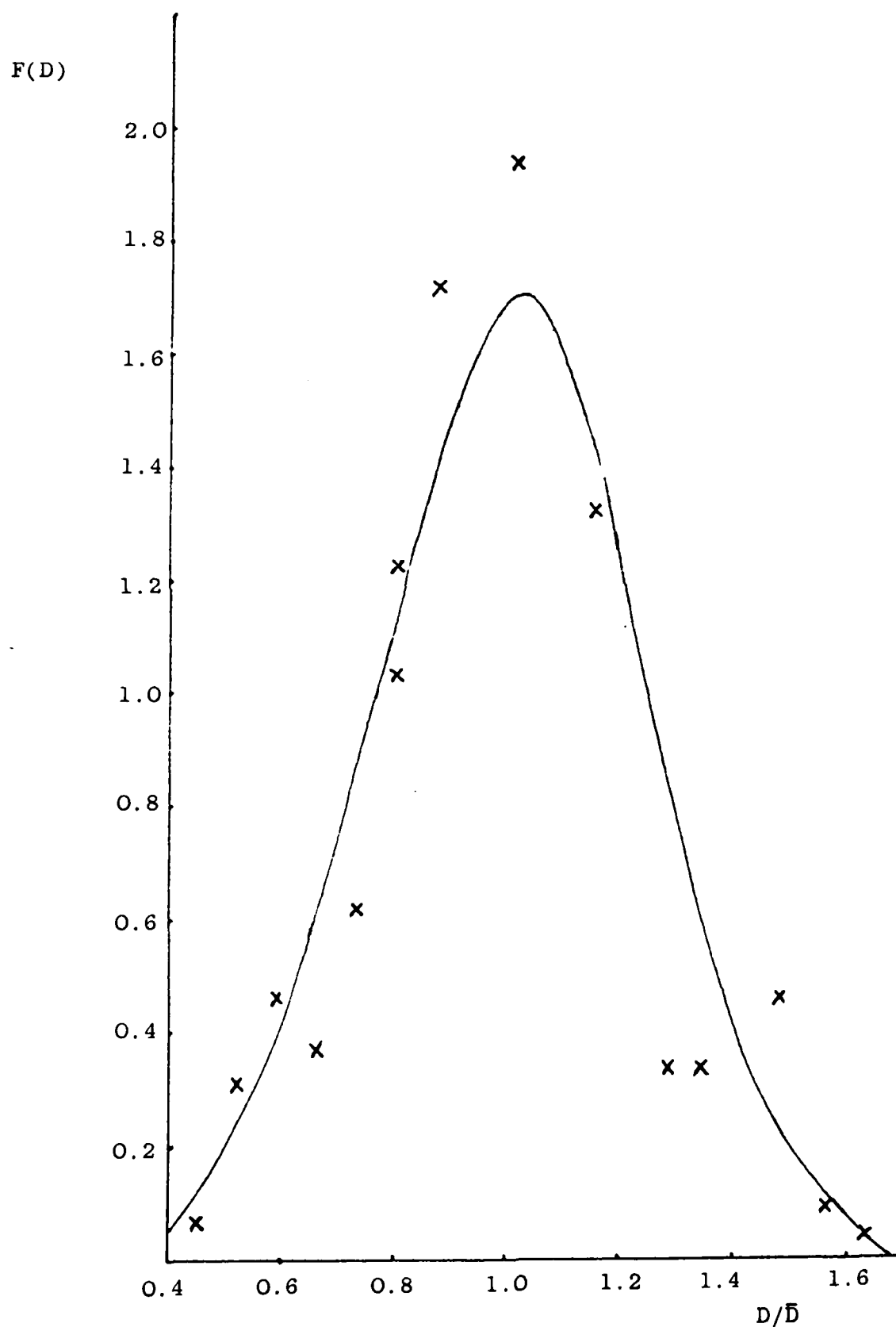


Fig. 3.1 Particle size distribution for a ferrofluid containing Fe_3O_4 particles. x-experimental measurement.

3 (b) Magnetic Measurements

The results which are discussed in this section were obtained for samples which contained cobalt particles dispersed in hydrocarbon carrier liquids. All of the experimental phenomena reported here are, however, equally applicable to ferrofluids containing either cobalt or magnetite particles.

3(b) (i) The Magnetisation Curve and Particle Size

Figure 3.2 shows two room temperature magnetisation curves for samples containing particles of average diameters $\bar{D} = 46\text{\AA}$ and $\bar{D} = 121\text{\AA}$. These two curves show a marked difference in the value of the initial susceptibility due to the fact that the energy of the particles in the applied field is dependent on the magnetic moment which in turn is proportional to D^3 . Also the approach to saturation for the smaller particle system is much more gradual due to the relatively larger effects of the thermal energy compared with the magnetic energy term.

Because of the marked variation in the form of room temperature magnetisation curves for different particle sizes it is possible to use data such as that shown in Figure 3.2 to determine the particle size distribution in the sample. This analysis was performed for each of the samples examined in this work using the well established technique due to Chantrell et al (1978), who give the median diameter of lognormal distribution of volume fraction

$$D_{vm} = \frac{18kT}{I'_s \pi} \left\{ \left(\frac{\chi_i}{3 I'_s} \cdot \frac{1}{H_0} \right)^{\frac{1}{2}} \right\}^{1/3} \quad 3.1$$

and standard deviation σ of $\ln D$

$$\sigma = \frac{1}{3} \ln \left\{ (3 \chi_i / I'_s \cdot (1/H_0)) \right\}^{\frac{1}{2}} \quad 3.2$$

where I'_s is the saturation magnetisation of the bulk material, χ_i is the initial susceptibility and $1/H_0$ is the intercept of a tangent to the high field data of an \bar{I} versus $1/H_0$ curve. The origin of these parameters are shown in Figure 3.3.

The data resulting from these calculations is shown in Table 3.1 together with the physical size parameters. Whilst the data obtained from electron microscopy and magnetic data has been fitted to different distributions the data is comparable since the standard deviations are small.

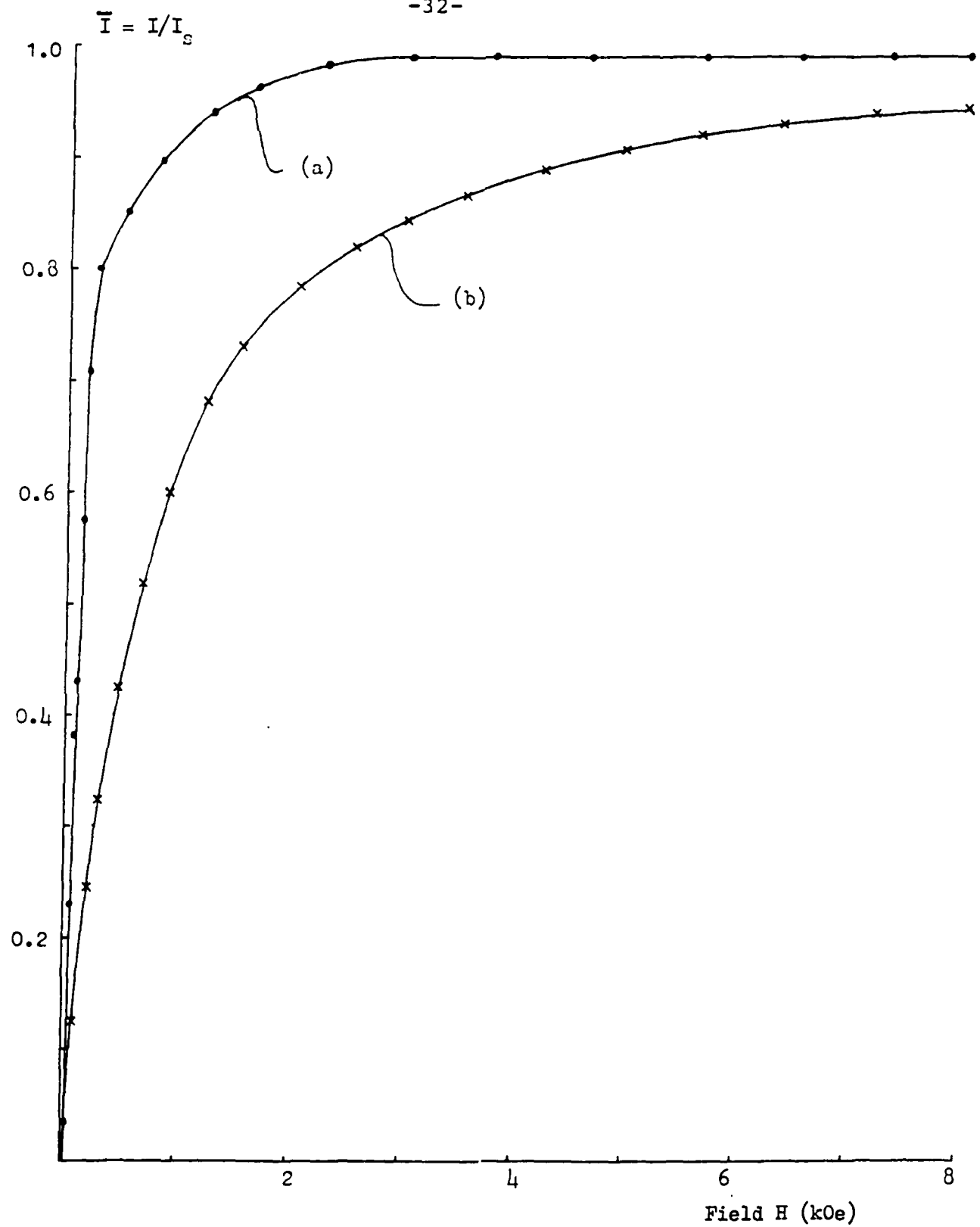


Fig. 3.2 Room Temperature (293°K) Magnetisation Curves for Cobalt Ferrofluids

(a) $\bar{D} = 121 \text{ \AA}$

(b) $\bar{D} = 46 \text{ \AA}$

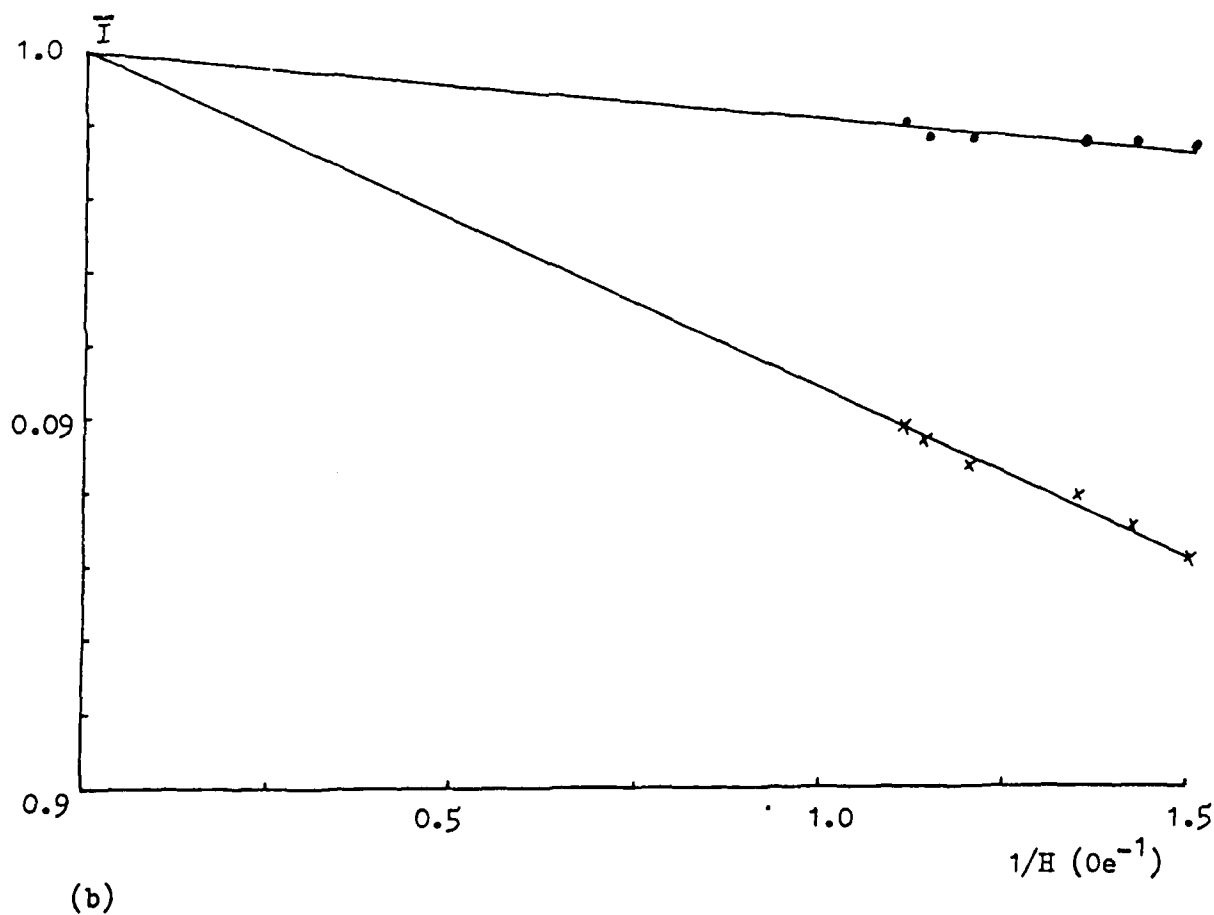
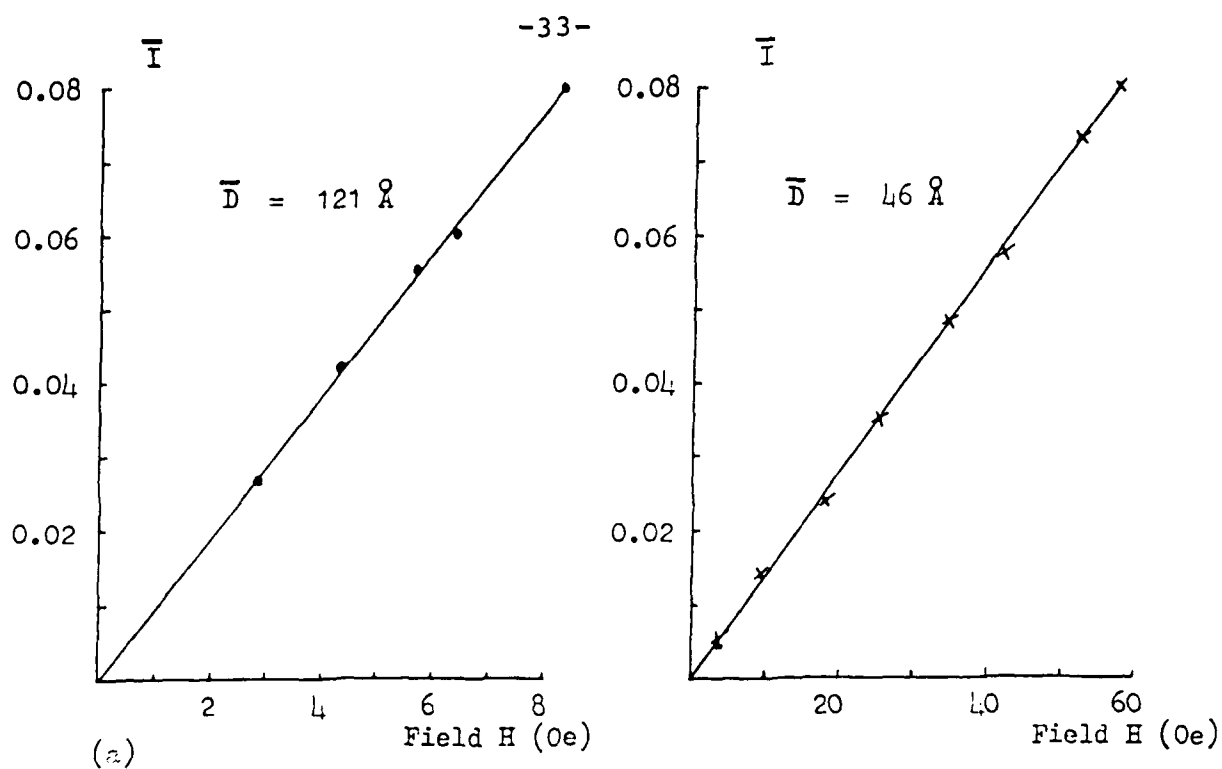


Fig. 3.3 Low and High Field Data

(a) The Initial Susceptibility, $\bar{\chi}_i$

(b) Saturation Magnetisation from $1/H$ Extrapolation

The difference between the data for physical and magnetic measurements is attributed to non-magnetic layers on the particles. For the case of those samples containing cobalt particles these non-magnetic layers are probably due to oxidation of the metal atoms. For the Fe_3O_4 particles the most likely origin is crystallographic defects or pinning of the spins of the atomic moments of the Fe^{2+} ions due to the bonding of the surfactant molecules (Berkowitz et al (1980)).

3(b)(ii) Superparamagnetic Behaviour of Ferrofluids

According to the theory of superparamagnetism magnetisation curves taken at different temperatures should superimpose when the magnetisation is plotted versus Field/Temperature (H/T). In Figure 3.4 (a) are shown three magnetisation curves for a ferrofluid containing cobalt particles of mean diameter $\bar{D} = 57 \text{ \AA}$ taken at three different temperatures.

In Figure 3.4 (b) this same data is shown plotted as \bar{I} versus H/T and the predicted superposition is observed, except at very low fields. This data is unique because only for a ferrofluid can true superparamagnetic behaviour be observed since the anisotropy energy is zero.

The small departures from true superparamagnetic behaviour in low field is attributed to the presence of dipolar interactions between the particles which in fact give rise to Curie-Weiss type behaviour. The low field insert in Figure 3.4(b) shows the general trend of the susceptibility.

3(b)(iii) Curie-Weiss Behaviour and Chain Formation

Figures 3.5 and 3.6 shows the variation of the reduced initial susceptibility $1/\chi_i (=1/(\chi/I_s))$ with temperature for the two ferrofluids containing cobalt particles with diameters $\bar{D} = 121 \text{ \AA}$ and 46 \AA . In each case a linear variation is observed. The extrapolation of the line strikes the temperature axis at a positive value in each case when $1/\chi_i = 0$. This temperature is denoted as T_0 , the ordering temperature.

The phenomenon of magnetic ordering in ferrofluids is not simply a magnetic ordering phenomenon but also involves the spatial ordering of the particles into long chains aligned in the field direction, which would be expected to give rise to significant optical and possible microwave anisotropy in the colloids. Unfortunately, all the ordering temperatures measured to date are below the freezing point of the carrier liquid used, but the data indicate that a significant proportion of the particles would be ordered at room temperature giving rise to similar effects.

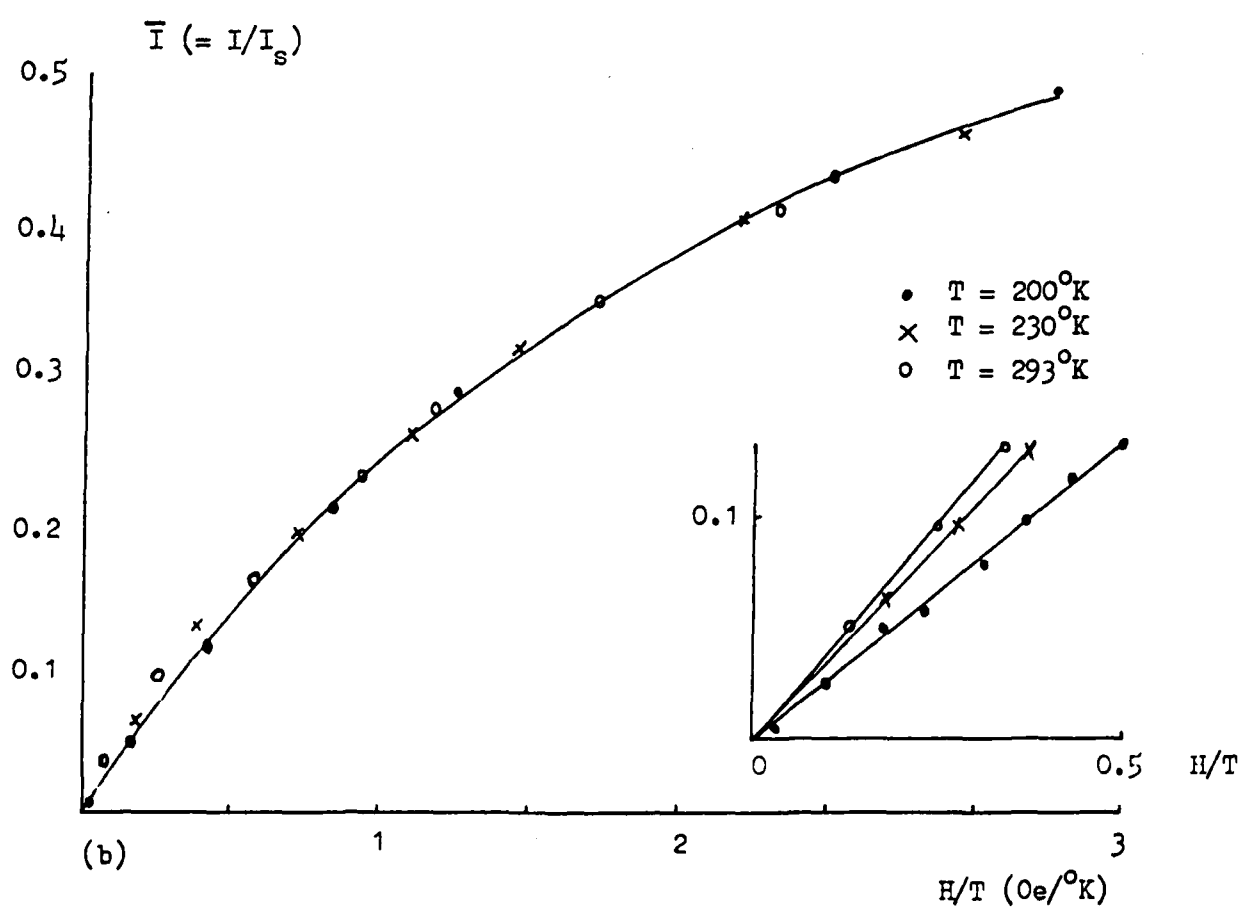
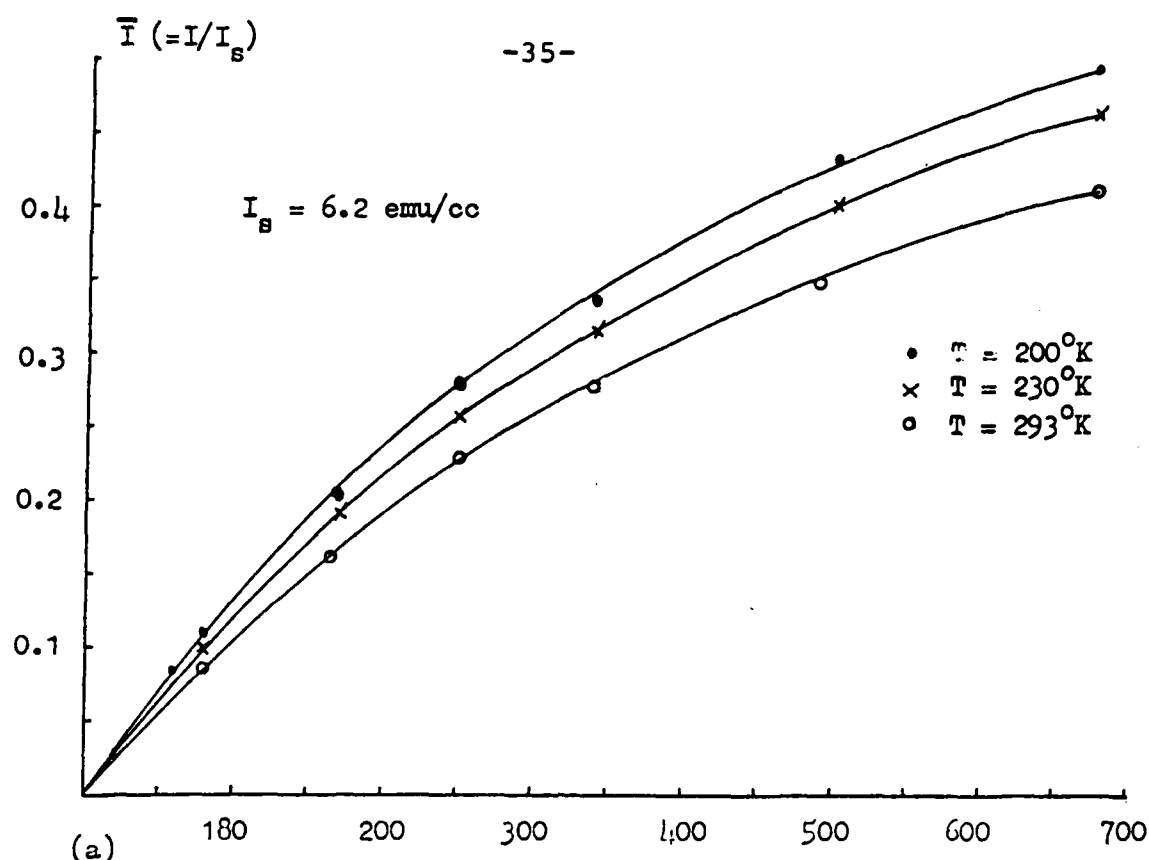


Fig. 3.4 Magnetisation Curves in the Liquid State
 (a) For $T = 293^\circ\text{K}$, 230°K and 200°K
 (b) Data from (a) showing H/T Superposition

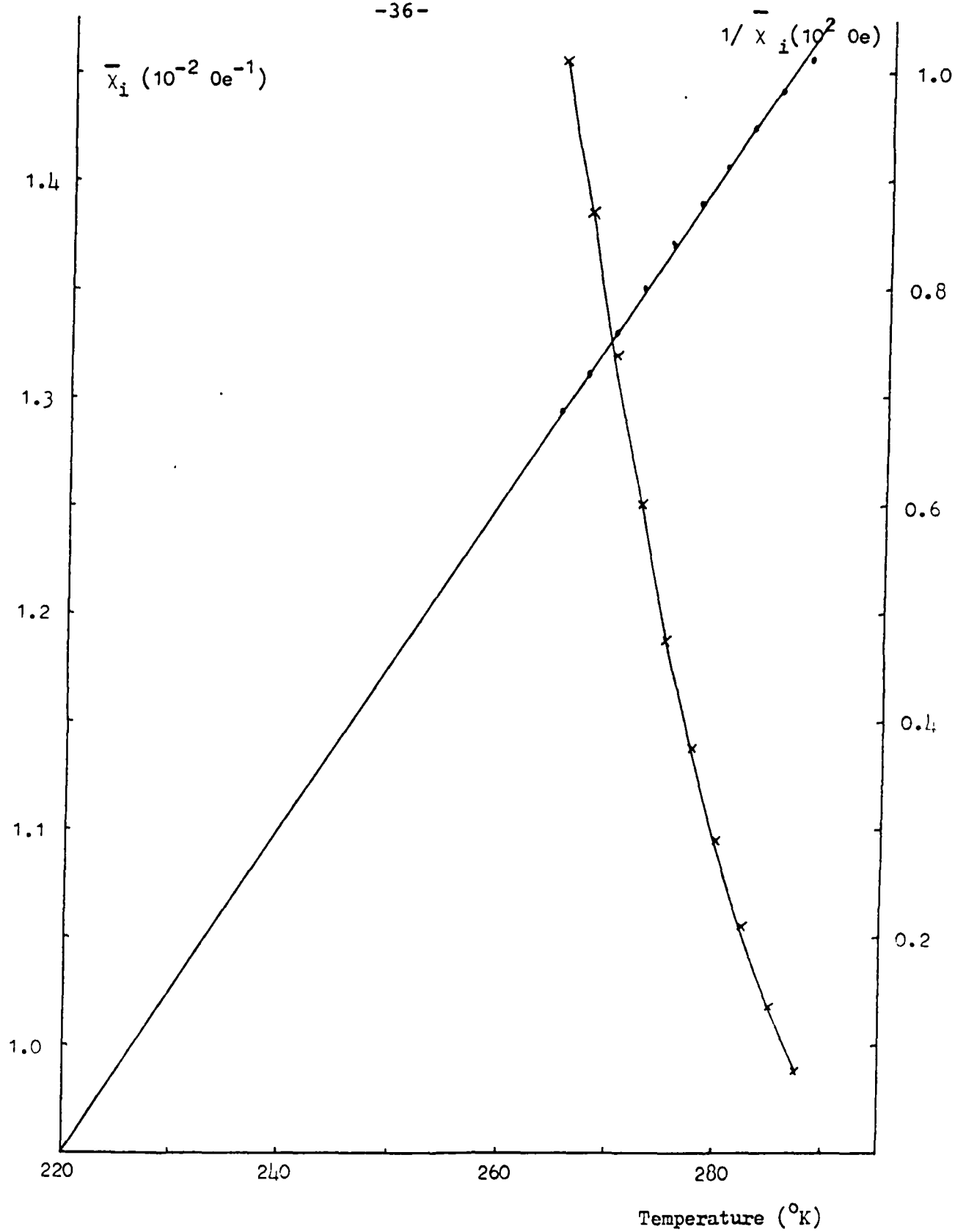


Fig. 3.5 $\bar{\chi}_i$ and $1/\bar{\chi}_i$ vs Temperature for a Sample with $\bar{D} = 121 \text{ \AA}$

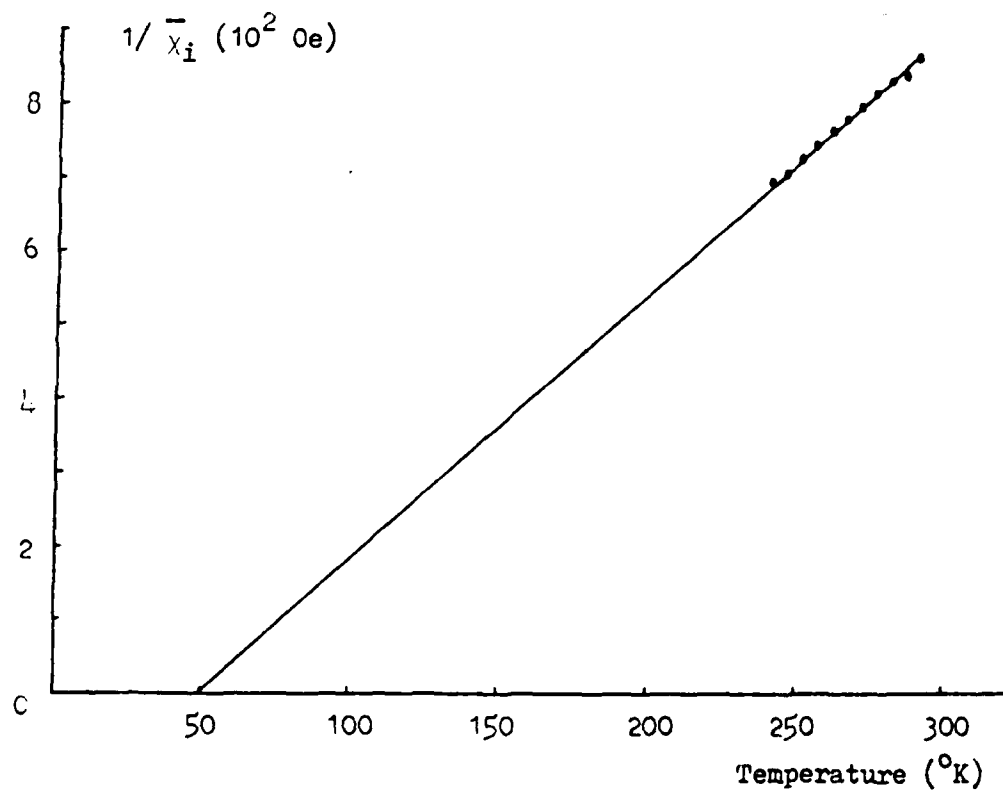
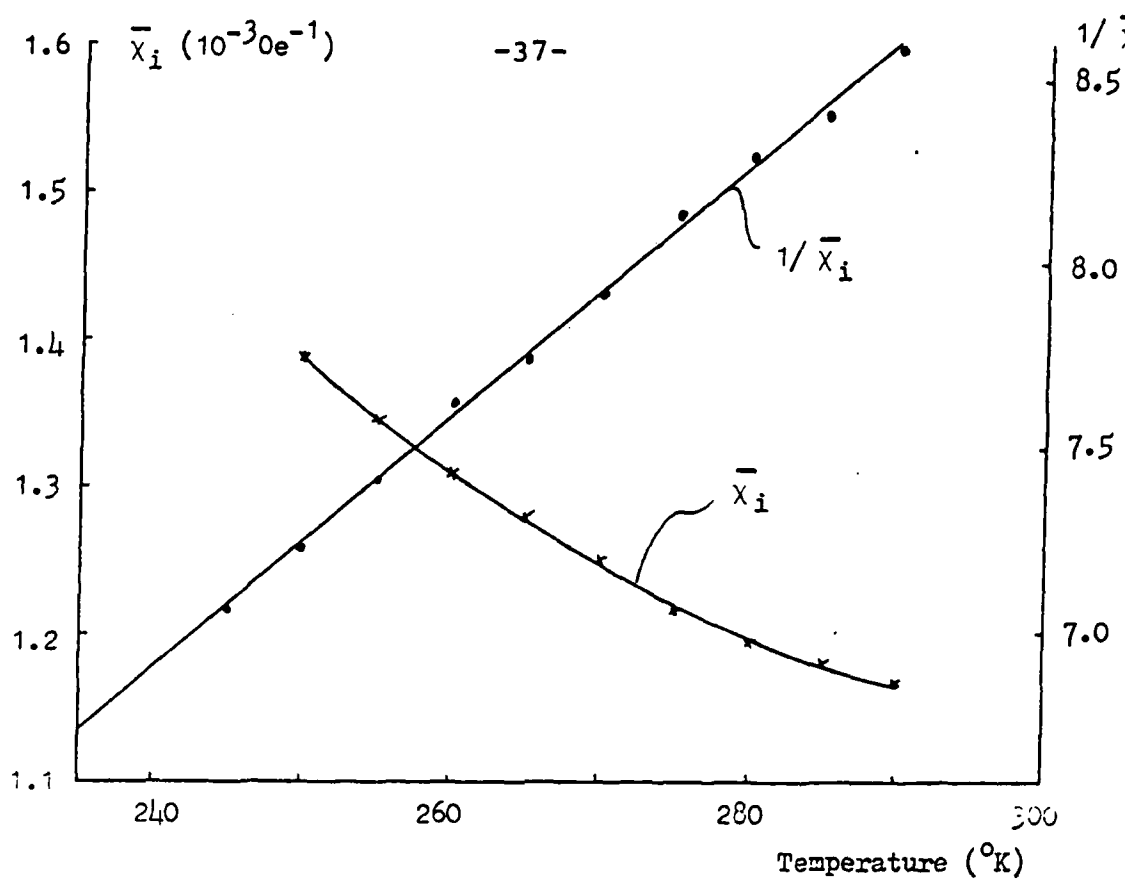


Fig. 3.6 $\bar{\chi}_i$ and $1/\bar{\chi}_i$ vs Temperature for a Sample with $\bar{D} = 46 \text{ \AA}$
 The lower graph shows the Extrapolation to $1/\bar{\chi}_i = 0$
 giving T_c .

Ordering of the magnetic particles whilst desirable for optical and microwave effects, may however, be detrimental to the colloidal stability of the colloids so an inevitable compromise is necessary.

The ordering of the ferromagnetic or ferrimagnetic particles in ferrofluids is also clearly analogous to the ordering of diamagnetic particles in the composite colloids. However, there is no obvious magnetic technique by which this ordering phenomena may be examined, (see Sections 3(b)(i) and 3(b)(ii)).

3(c) Thin Film and Concentration Measurements

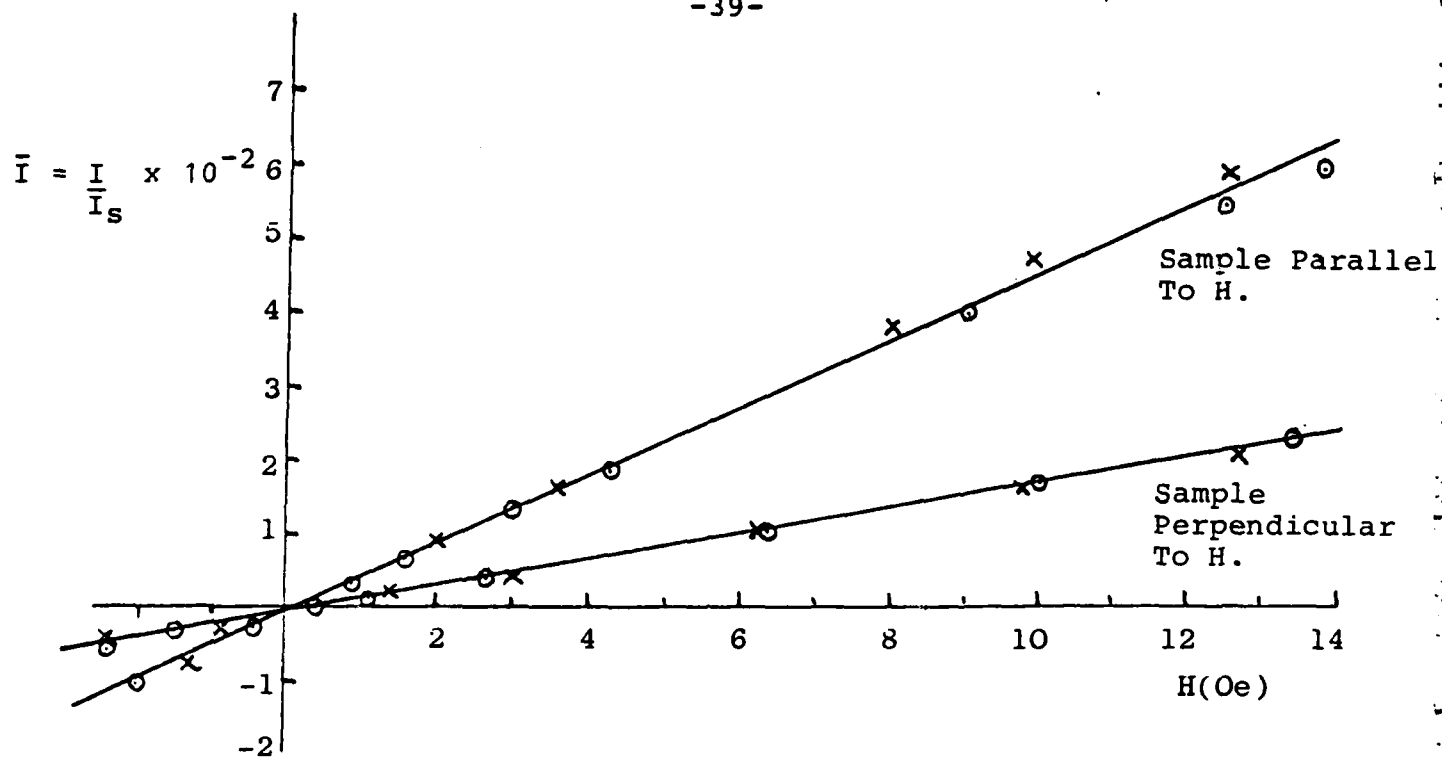
3(c)(i) Thin Films of Ferrofluids and Composite Colloids

Samples of thin films of ferrofluid and composite colloids were prepared using the method given in Section 2(b)(i). It was thought that the presence of a high concentration of large (compared to the size of the ferrofluid particles), diamagnetic spheres could influence the magnetic behaviour of the films. Four samples were made, two containing a 515 G ferrofluid, the other two containing the same ferrofluid and a high concentration of 10.0 μ m polystyrene spheres. Two magnetisation curves with the long axis of the samples parallel and perpendicular to the applied field were measured for each sample; plots are shown in Figure 3.7(i) and (ii). As can be seen the two Figures are very similar.

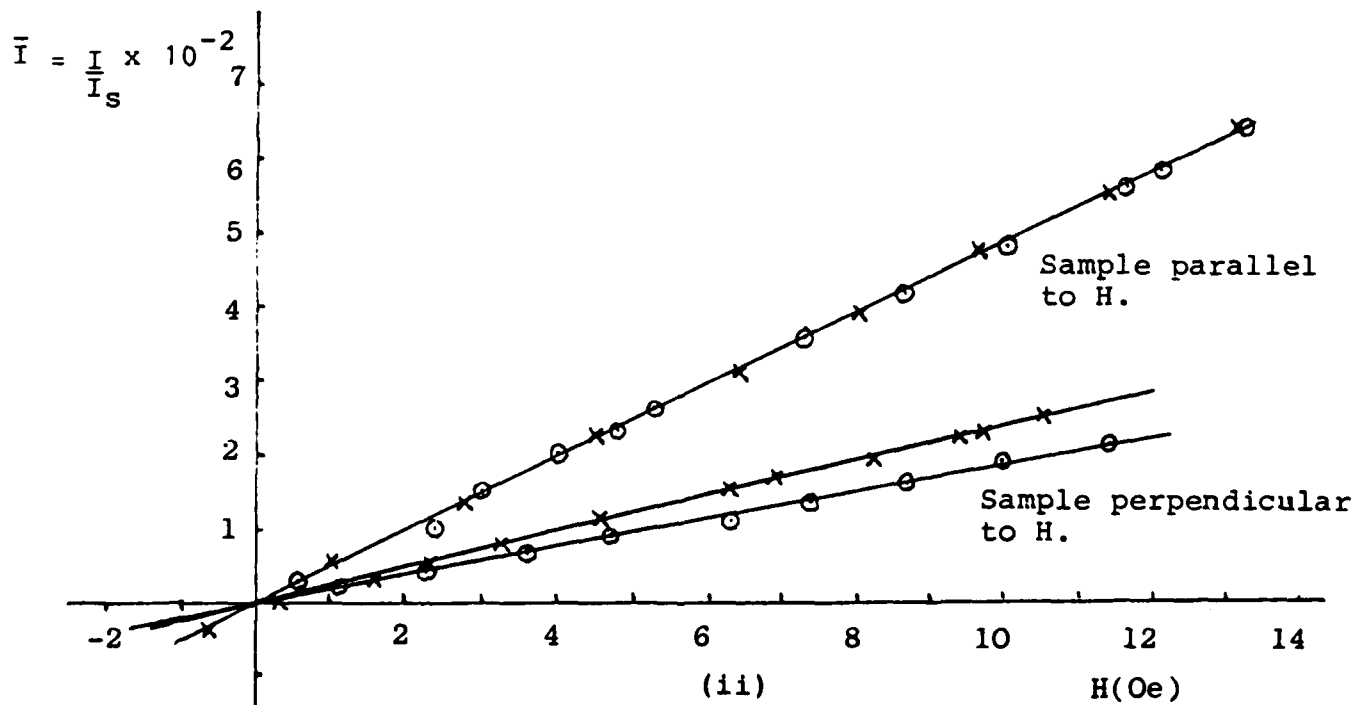
Taking Figure 3.7(i) it is clear that the presence of the spheres in the samples has no effect on the magnetisation of the fluid. The curve measured parallel to the field for the samples containing spheres superimposes upon the curve measured parallel to the field containing ferrofluid alone and this is repeated in the field perpendicular case.

However, the data does show an unexpected anisotropy in the samples. Even after applying the maximum demagnetizing factor of 4π to the curves of the samples measured with their long axis perpendicular to the field, superposition with the parallel case does not occur. The low field results show a large decrease in initial susceptibility, χ_i for the field perpendicular case. It is evident from Figure 3.7(i) that χ_i has been reduced to about 38% of the parallel field value. At high fields non-superposition is repeated with the magnetisation value of the films measured perpendicular to the field some 30% lower than when measured parallel to the film.

The reason for this difference in magnetisation curve for the same fluid is still unclear. In each case the curves were measured with the film parallel to the field first and then the



(i)



(ii)

Fig.3.7 Magnetisation curves of thin film colloids
 ○ ≡ Ferrofluid
 X ≡ Composite Colloid.

sample was rotated through 90° to measure the perpendicular case. This could result in the chains of ferromagnetic particles formed in the field, bonding to the glass surface in some way. If this were the case then upon orientation of the sample some chains could remain bonded to the glass and they would not contribute to the magnetisation in the field direction except at very high fields. Some evidence of this occurring has been put forward by Taketomi (1983). He suggest that chains form in thin films of ferrofluid near the glass surface of the sample.

3(c)(ii) Measurement of Concentration of Spheres in a Ferrofluid.

Magnetisation curves were measured on two magnetometer buttons, one containing ferrofluid alone, the other containing the same ferrofluid and $10.0\mu\text{m}$ polystyrene spheres. Figures 3.8(i) and (ii) show the low field region of these curves; in Figure 3.8(i) magnetisation has the units of emu per g and in Figure 3.8(ii) it is expressed in reduced units.

The two plots in Figure 3.8(i) do not superimpose i.e. the initial susceptibility of the sample containing spheres is less than for the fluid alone. This is to be expected since the mass of the spheres contributes to the mass of the sample but not to its magnetisation.

If we let V_B be the volume of fluid in sample B (containing fluid alone), V_A the volume of fluid in sample A (containing fluid and spheres), χ_B the initial susceptibility of sample B and χ_A the initial susceptibility of sample A then

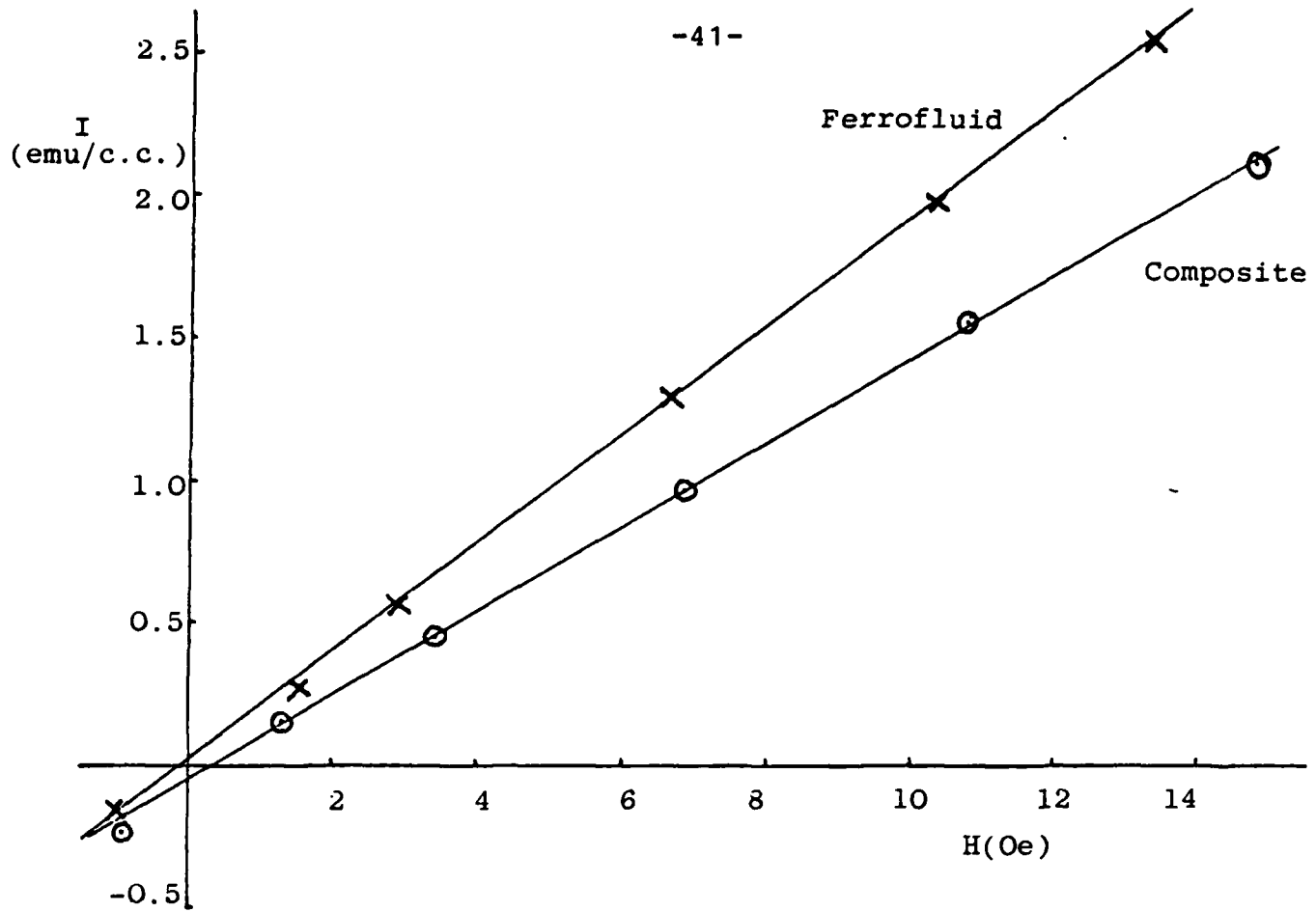
$$\frac{V_A}{V_B} = \frac{\chi_A}{\chi_B} \quad 3.1$$

$$\text{i.e. } V_A = \frac{V_B \chi_A}{\chi_B} \quad 3.2$$

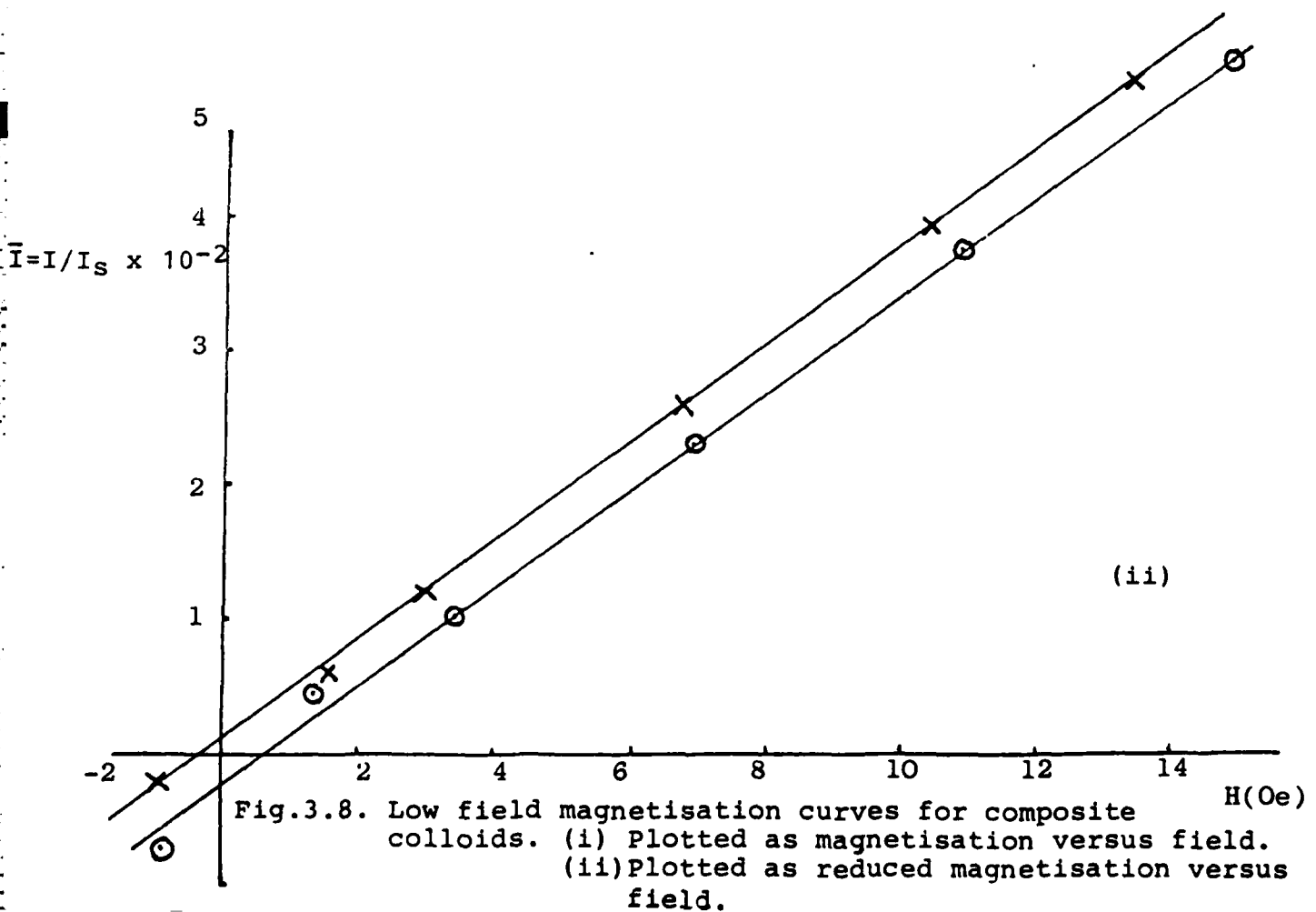
Now $V_B - V_A = V_{SB}$ will be equal to the volume of spheres in a volume of fluid equivalent to V_B . Using equation 3.2.

$$V_{SB} = V_B - V_A = V_B - \frac{V_B \chi_A}{\chi_B}$$

$$\text{i.e. } V_{SB} = V_B \left(1 - \frac{\chi_A}{\chi_B} \right)$$



(i)



(ii)

Fig.3.8. Low field magnetisation curves for composite colloids. (i) Plotted as magnetisation versus field. (ii) Plotted as reduced magnetisation versus field.

Now the volume of spheres per c.c. of fluid will be

$$\frac{V_{SB}}{V_B} = V_{SC} \quad 3.4$$

$$\text{i.e. } V_{SC} = \frac{V_S}{V_B} = V_B \left(1 - \frac{\chi_A}{\chi_B}\right) / V_B = 1 - \frac{\chi_A}{\chi_B} \quad 3.5$$

The number of spheres per c.c. of fluid, N, will be V_{SC} divided by the volume of one sphere

$$\text{i.e. } N = V_{SC} / \frac{\pi d^3}{6} = \text{concentration of spheres per c.c.}$$

where d = diameter of a sphere (10.0 μ m)

$$\text{i.e. } N = \frac{6 V_{SC}}{\pi d^3} = \frac{6}{\pi d^3} \left(1 - \frac{\chi_A}{\chi_B}\right) \quad 3.6$$

Taking $\chi_A = 0.146$ and $\chi_B = 0.183$ emu/c.c./Oe from Figure (i) we have

$$N = \frac{6}{\pi \times (10 \times 10^{-4})^3} \cdot \left\{1 - \frac{0.146}{0.183}\right\} \quad 3.7$$

$$\text{i.e. } N = 3.9 \times 10^8 \text{ spheres per c.c.}$$

This value is in agreement with calculations made from Plate 3, Section 3(e).

This method can be used to measure the concentration of spheres in any composite colloid provided the spheres used are uniform in size. This method will be useful where measurements are made on samples containing different concentrations of spheres.

Figure 3 8(ii) shows the low field reduced magnetisation curve. The two plots are parallel which would be expected using reduced units since the presence of the spheres has now been taken into account. The two curves do not superimpose exactly due to a small offset in the Hall probe between readings.

3(d) Diffraction Measurements

As outlined in Section 1(d) a random array of spheres will act as a single circular aperture of diameter d , where d is the diameter of the spheres. A composite colloid sample containing a monolayer of $10.0\mu\text{m}$ polystyrene spheres in a hexadecene based ferrofluid ($M_s = 400\text{ G}$) was illuminated by a 1mW helium-neon laser as described in Section 2(f).

The diffraction pattern observed is shown in Plate 2. The pattern is circularly symmetric and consists of the bright central Airy disk surrounded by concentric circular bands of rapidly decreasing intensity.

With a low ($\sim 100\text{ Oe}$) uniform field parallel to the film i.e. perpendicular to the light path, the spheres align. The diffraction pattern resulting from this alignment is shown in plate 2(lower). For a completely regular grating the diffraction pattern would be sharply defined. However, there is a slight non-uniformity in the diffraction grating caused by different thicknesses of surfactant on the spheres and minor impurities in the sample. Also, the grating is made up of curved apertures rather than square or rectangular ones. The above factors all give rise to a slight loss of definition in the pattern. The measurements were repeated using a similar sample containing $4.7\mu\text{m}$ spheres. The results of the two experiments can be seen in Table 3.2 and show excellent correlation with the manufacturer's nominal diameter.

Manufacturer's Nominal Diameter (μm)	Diameter from Diffraction Expts. (μm)	
	Zero Field	Low Field
10.0	9.9 ± 0.2	10.0 ± 0.2
4.7	4.6 ± 0.2	4.7 ± 0.2

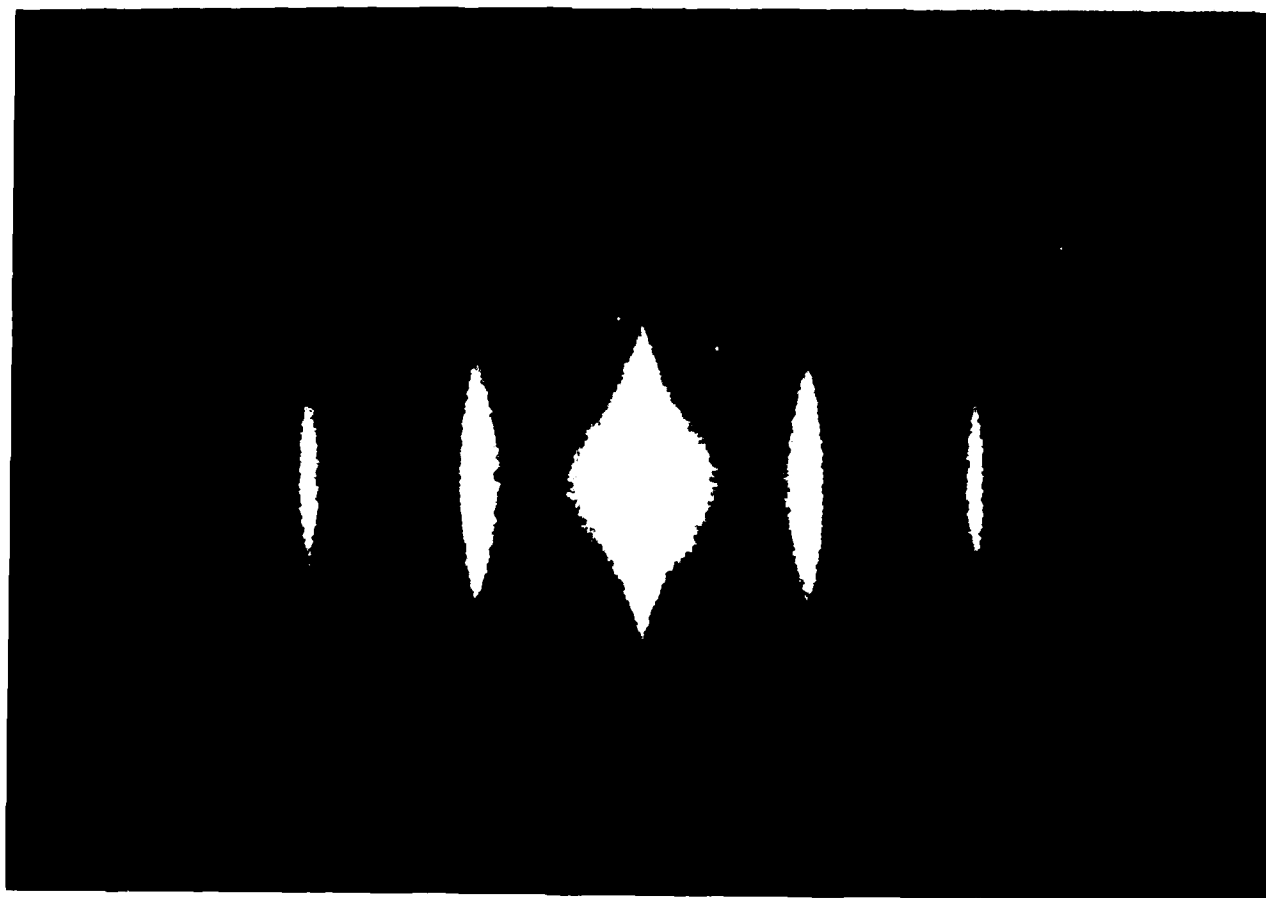
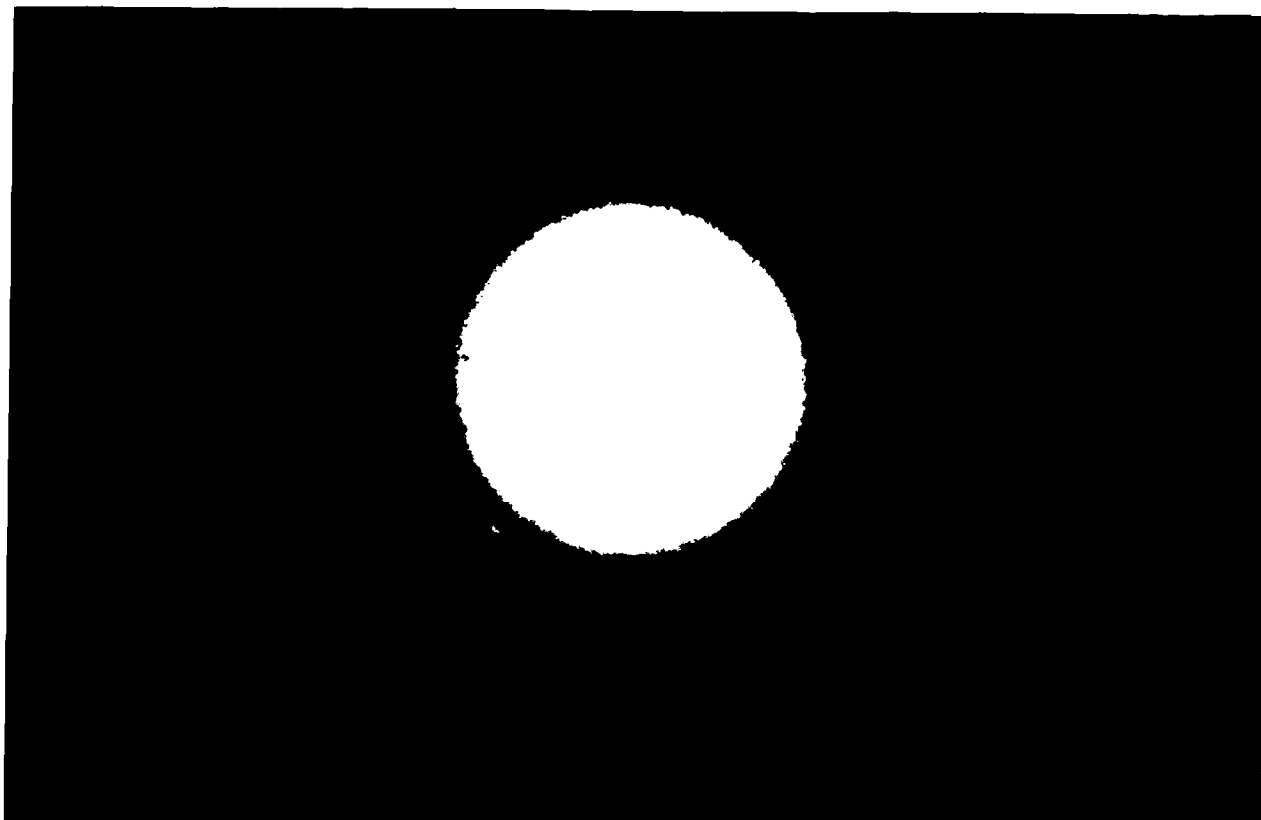
Table 3.2

Superimposed upon the latter diffraction pattern is another central, vertical straight line; this is the diffraction pattern due to the ferrofluid alone as observed by Haas and Adams (1975). The pattern is due to a chaining of the ferromagnetic particles under the influence of the magnetic field.

Plate 2. Diffraction Patterns of a Composite Colloid

Top : Zero Field

Bottom : Field = 100 Oe, direction \longrightarrow



3(e) Micrographs of Composite Colloids

Plate 3 shows four photographs, taken on a Swift MP120 polarizing microscope, of 10.0 μ m polystyrene spheres in a ferrofluid. The top right hand photograph is of the sample in zero field. The spheres are randomly aligned and little or no spatial order is apparent, which is to be expected. In the top left hand photograph, a small field (~ 100 Oe) has been applied parallel to the sample. The spheres have acquired an apparent attractive magnetic moment (Section 1(b)) and have formed chains of up to 40-50 spheres in the direction of the field. Even longer chains have been observed by applying higher fields (>200 Oe) over a period of some time. If the direction of the field is changed slowly then the chains will couple to the field and change direction with it. However, with a more rapid change of field, the chains break into trimers and dimers, only to reform into long chains once the field is stationary again. Apparatus has recently been completed at Bangor to study samples under the microscope in rotating field conditions.

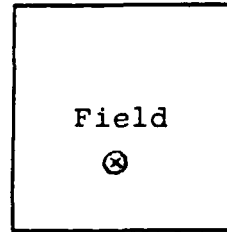
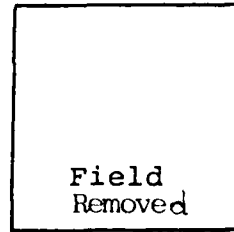
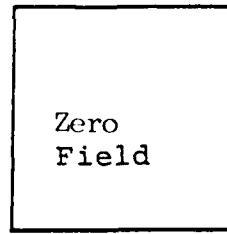
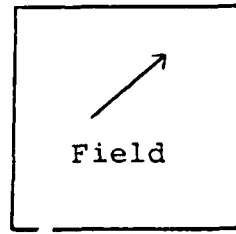
The bottom right hand photograph shows the sphere configuration with an applied field of about 50 Oe perpendicular to the sample i.e. into the plane of the photograph. The spheres have acquired an apparent repulsive magnetic moment and have formed a two-dimensional triangular lattice. There are a few dislocations due to slight impurities in the sample and spheres sticking together. However, with very clean samples and higher fields a truly regular lattice is obtained.

The bottom left hand photograph shows the chains about 1-2 seconds after the field parallel to the sample has been removed. Comparing this picture with the top right hand photograph it is evident that on removal of the field, the system, which is under a field induced "tension" relaxes immediately to the state shown in the photograph below. However, the time taken for the system to reach a state similar to the top left hand photograph by diffusion is a matter of days, showing that Brownian motion effects on the comparatively large spheres is slight.

Plate 4 shows a series of photographs of the most recent and potentially most useful application. The photographs are of a thin film of composite consisting of tin powder in a decalin based ferrofluid (Section 2(h)). The top photograph shows the tin particles (dark areas) randomly arrayed in zero field. However, upon application of a field the anisotropic particles line up in chains with their long axis parallel to the field (middle photograph). The final photograph is of a different sample containing a higher concentration of tin particles.

By introducing conducting particles into the ferrofluid the possibilities of using the system as a polarizer are improved. Experiments to observe metallic non-magnetic powders, of different sizes, shapes and concentrations are underway.

Plate 3. 10.0 μm Spheres in a Ferrofluid.



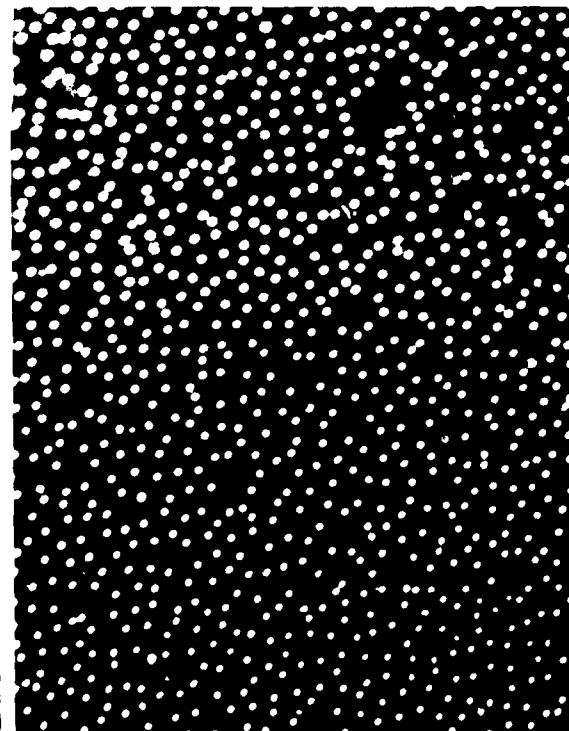
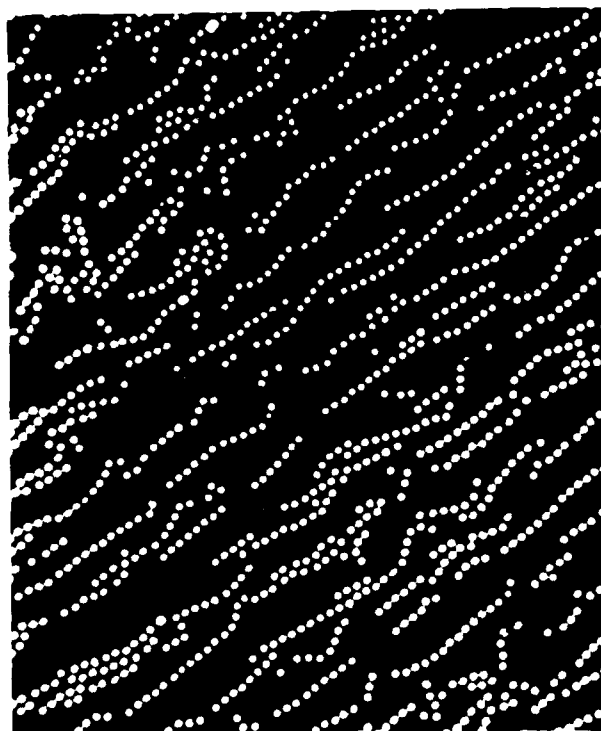
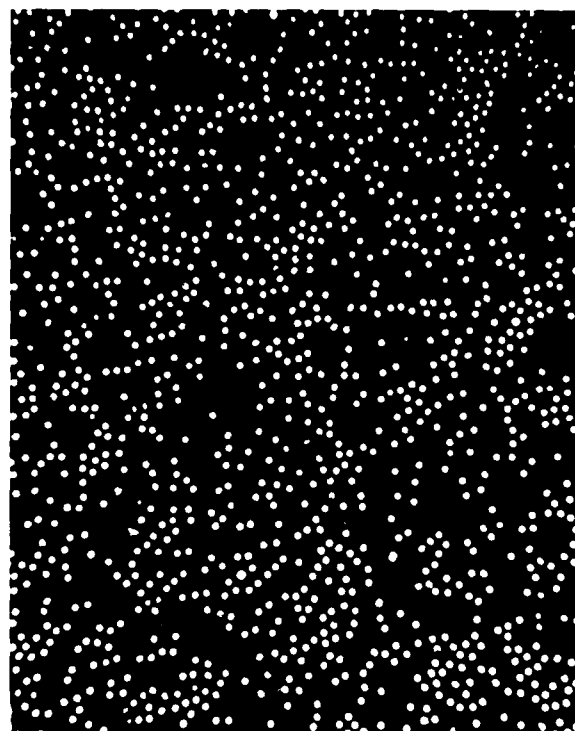
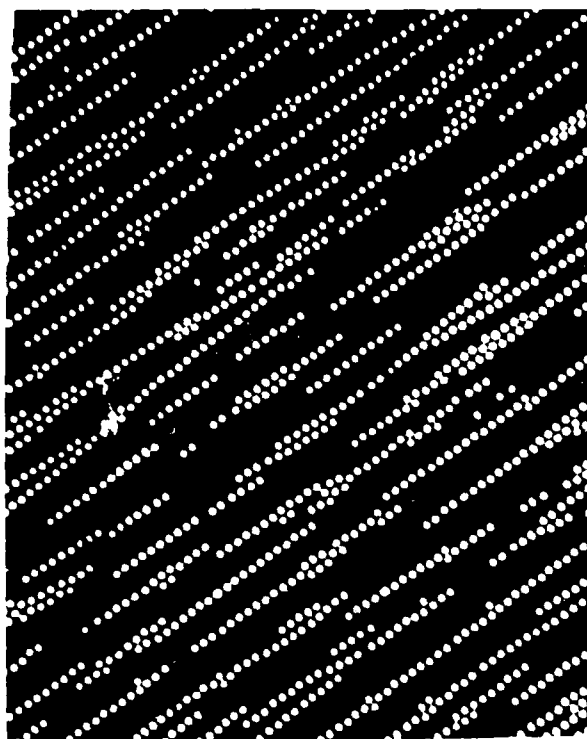
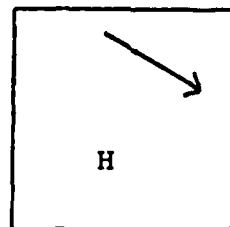
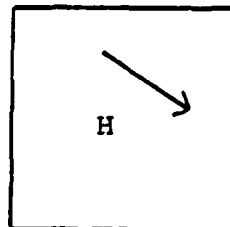
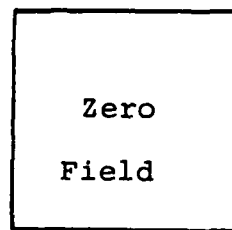
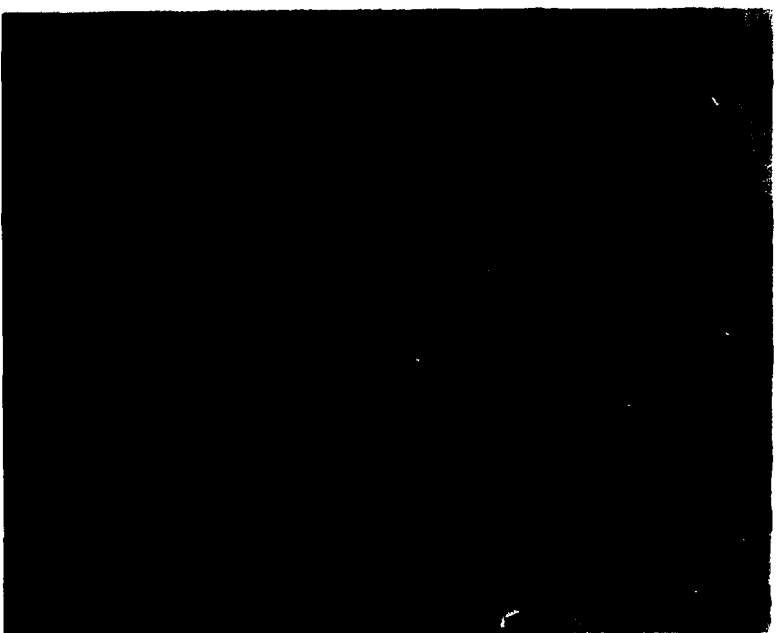


Plate 4. Tin Particles in a Ferrofluid.





3.(f) Observation of Labyrinthine Instability

Plate 5 is a series of photographs showing the "growth" of the labyrinthine pattern that forms at the interface of a ferrofluid and an immiscible liquid.

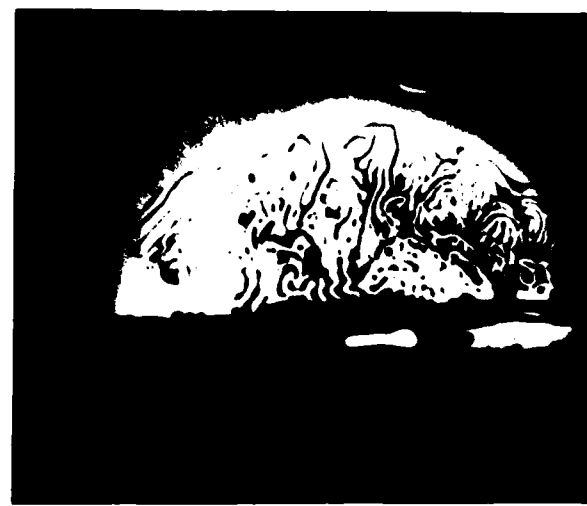
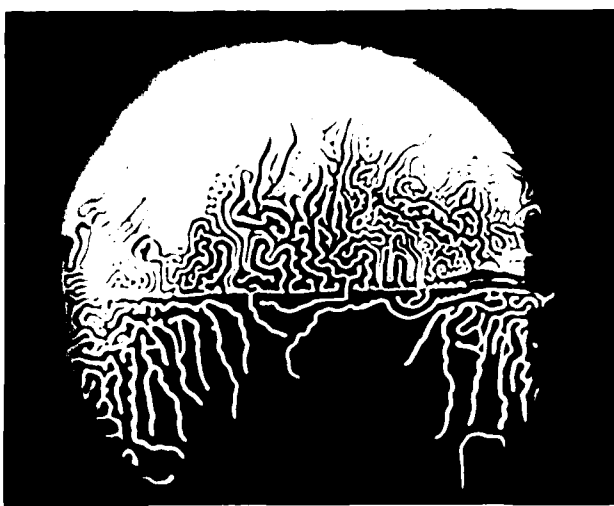
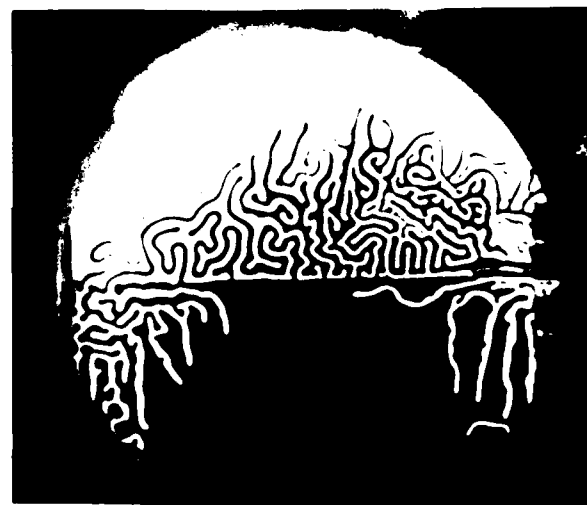
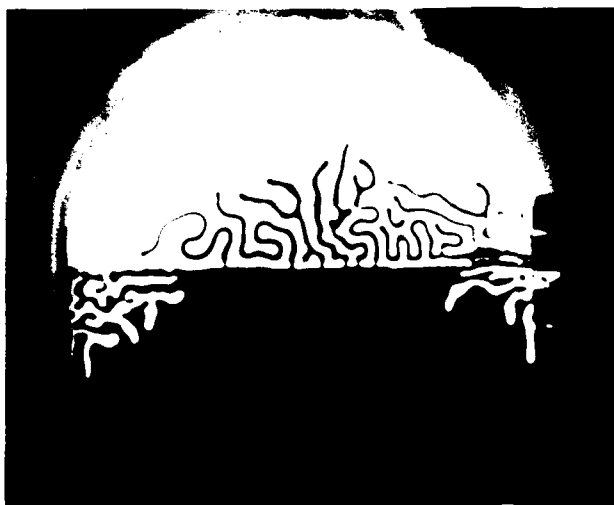
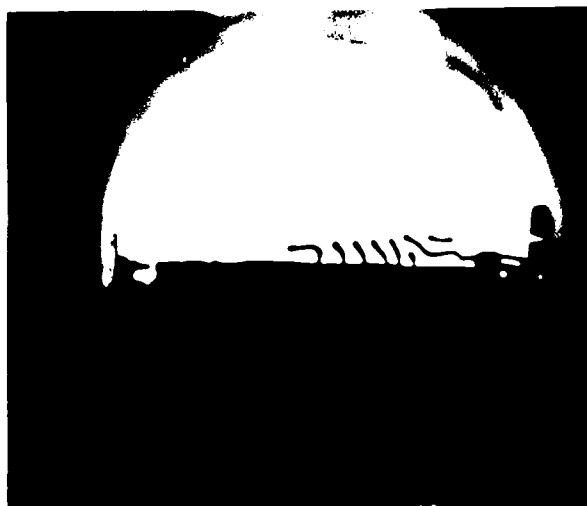
The top left hand photograph is the cell in zero field, the bottom, dark layer is the ferrofluid and the clear liquid above it the less dense immiscible aqueous phase. The field is increased until at about 100 Oe a slight invasion into the aqueous phase by the ferrofluid occurs. This is shown in the top right hand photograph. As the field is increased to about 150 Oe the invasion increases (middle left hand picture); the single "fingers" of magnetic liquid bifurcate and lengthen, as do the thicker fingers of the water. The middle right hand photograph shows the patterns at maximum field of the electromagnets i.e. ~ 350 Oe. The pattern has become highly convoluted and complex and the growth of fingers is slow. However, after the field had been left on for three hours the pattern shown in the bottom left hand corner formed. The pattern was in equilibrium after this time since no change could be detected after a 24 hour period. After this period the field was removed and the labyrinthine pattern allowed to relax. The final photograph in the sequence shows the system in relaxed state. As can be seen some annealing occurs and the fluids do not revert to their original state.

3(g) Optical Birefringence Results

The anisotropy introduced into the three composite samples by the chaining of the polystyrene spheres did not induce any birefringence in the light passing through the sample. When a field was applied to any of the three samples used in these measurements the output meter registered a deflection. This indicated that birefringence was present in the sample. However, in all cases, the birefringence decayed rapidly when the field was removed. This suggests that the birefringence was caused by the fluid alone, since the chains of spheres do not become randomly aligned quickly on the removal of the field, but remain ordered to a certain extent for much longer time periods (Section 3(d)). The magnetic particles will, on the other hand, take a time of the order of milliseconds to relax.

These birefringence measurements suggest that the chains formed by even the smallest of the polystyrene spheres ($d=0.22\mu\text{m}$) are too large to produce birefringent effects at optical frequencies.

Plate 5. Labyrinthine Instability in a Ferrofluid.

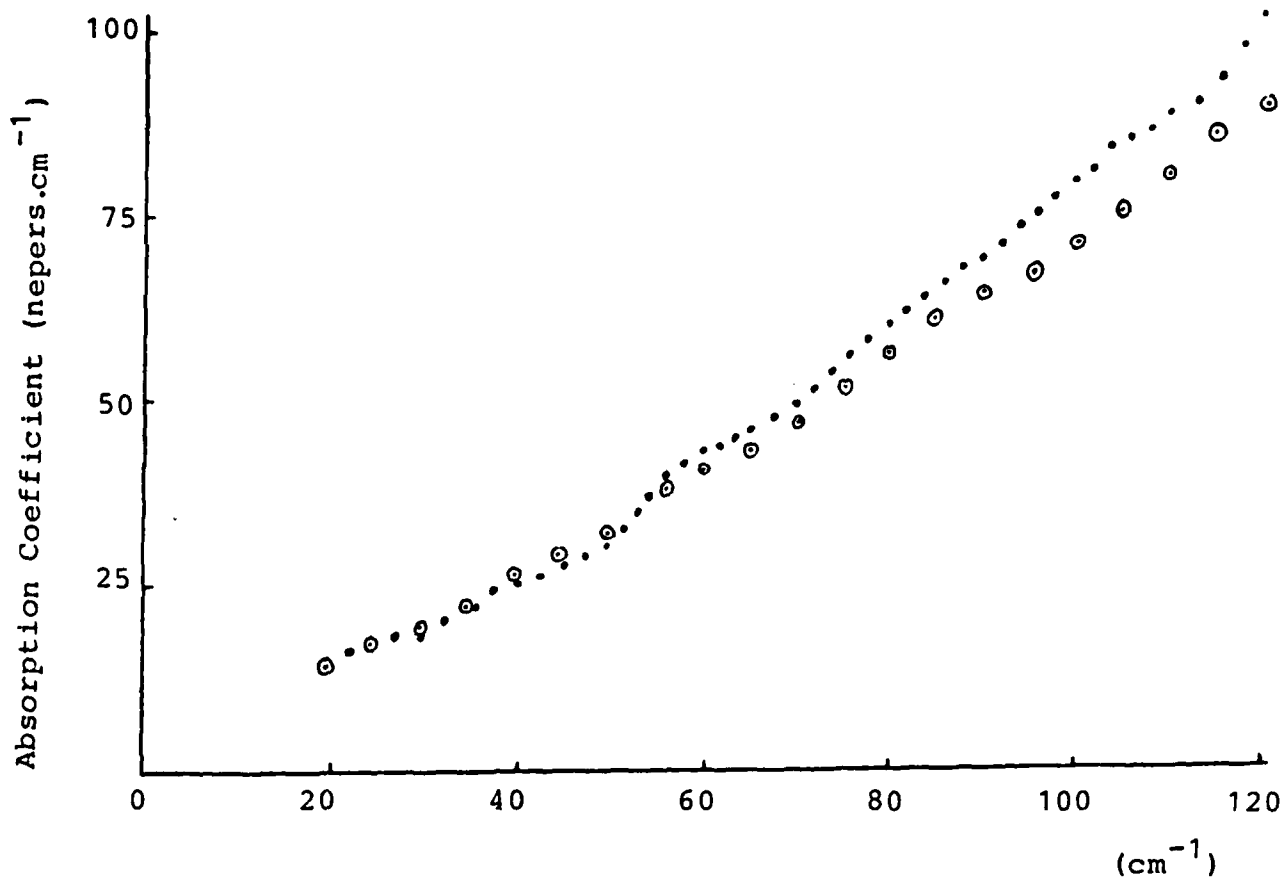


3(h) Microwave Results

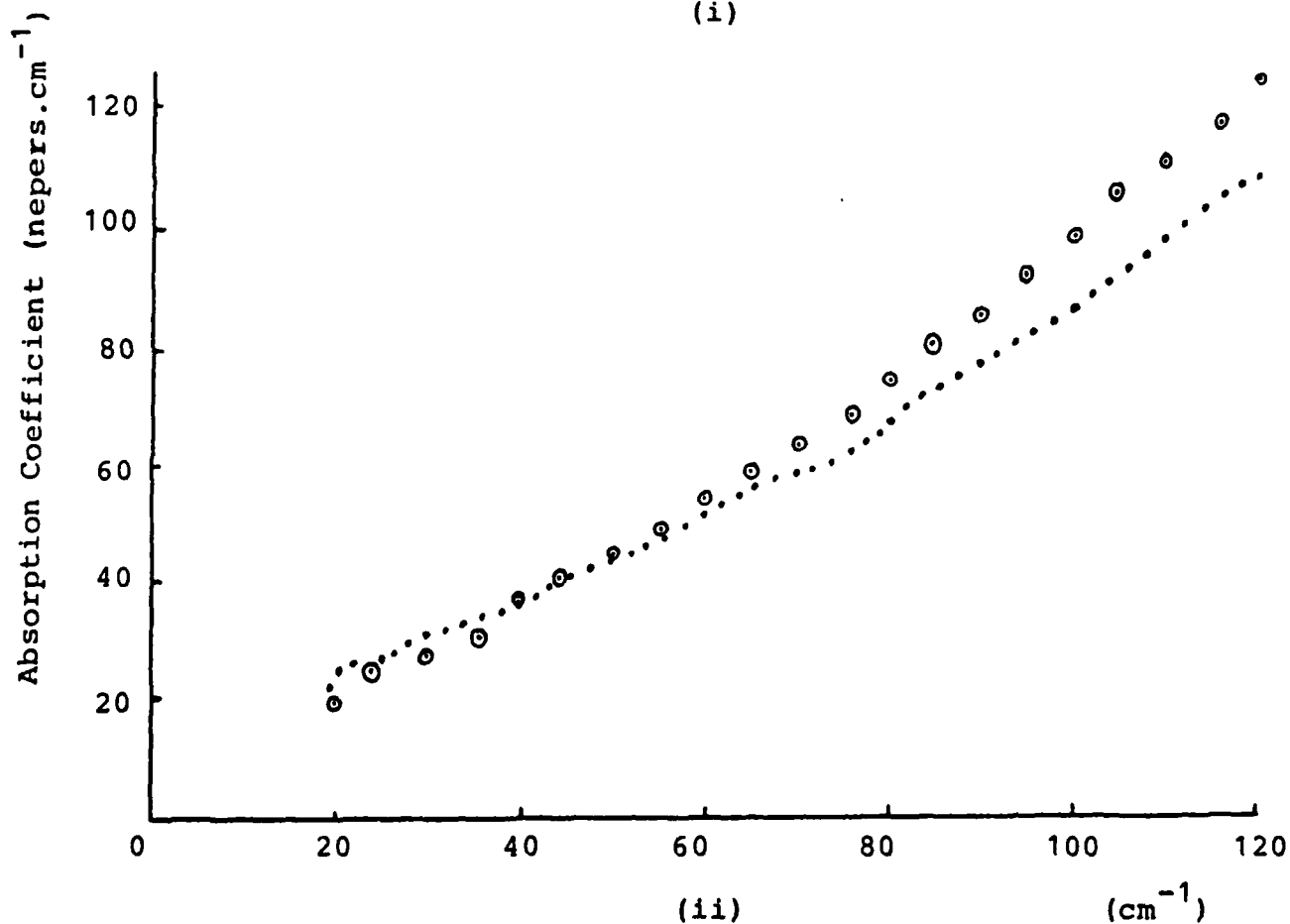
Figure 3.9(i) shows the absorption - wavelength characteristics of a decalin based magnetic ferrofluid ($M_s=600G$) with and without an applied field of $6KOe$. The field was applied parallel to the sample, i.e. perpendicular to the radiation of the system. As can be seen there is an appreciable change in absorption when the field (Figure 3.10(i)) is applied to the sample. At about 120 cm^{-1} the absorption of the fluid is significantly lower with a field applied, than in zero field, i.e. a dichroism is magnetically induced in the sample. This change however is wavelength dependent and decreases with wavelength.

Figure 3.9(ii) also shows a change in absorption on application of a magnetic field. The sample was the same 600 G ferrofluid containing glass spheres ($d=5\pm 3\mu m$). Glass was used since it absorbs strongly in the wavelength range required; polystyrene, however transmits to a certain extent in the microwave region. The magnetic field in this case was approximately 500 Oe and was applied perpendicular to the sample i.e. parallel to the radiation of the spectrometer (Figure 3.10(ii)). The field is a factor at 12 lower than in the previous example but an appreciable effect is again observed. However, with glass spheres present and the field perpendicular to the sample the effect is reversed; i.e. with a field present the absorption of the sample is higher than in zero field. At higher wavelengths, however, the two plots converge.

These preliminary results are interesting and a programme of measurements has been planned on a variety of different systems.

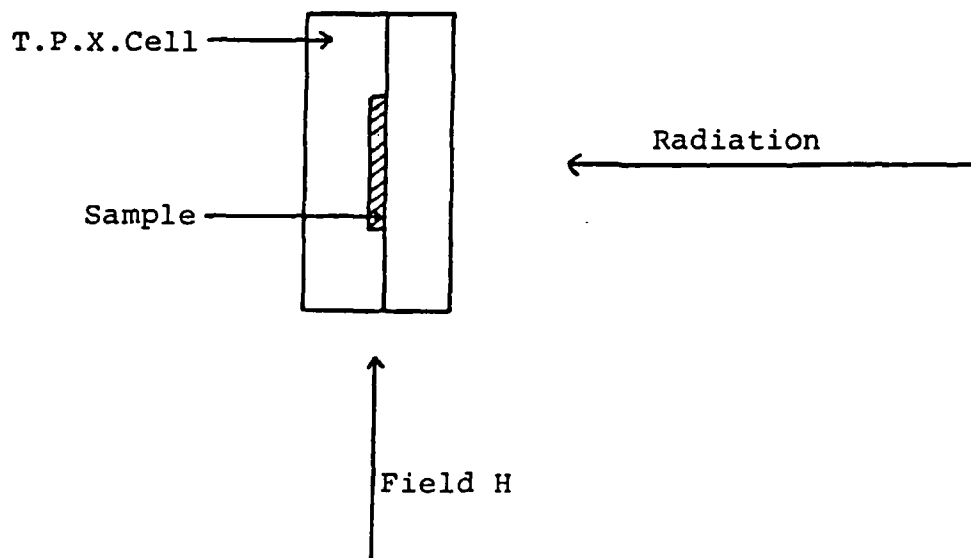


(i)

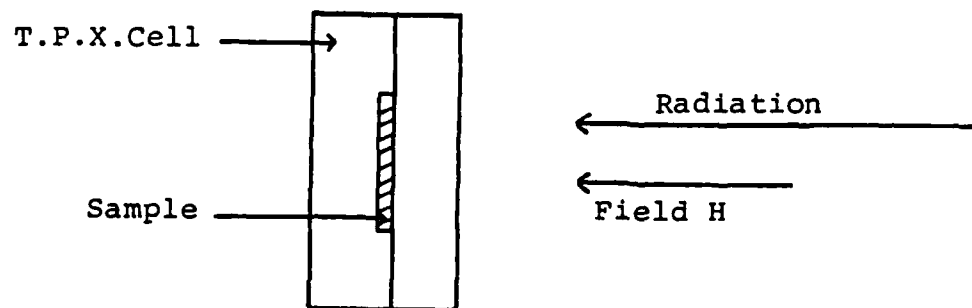


(ii)

Fig.3.9 (i) 600G ferrofluid; · zero field, ⊙ Field=6kOe parallel to sample
(ii) 600G ferrofluid and glass spheres; · zero field, ⊙ field=500 Oe perpendicular to sample.



(i)



(ii)

Fig.3.10 (i) Orientation of Cell for Microwave Experiment 1
(ii) Orientation of cell for Microwave Experiment 2

4.

CONCLUSIONS AND RECOMMENDATIONS

A number of materials based on ferrofluids have been prepared and studied. The different material types can be categorised as

- (i) Colloidal dispersions of cobalt or Fe_3O_4 particles;
- (ii) Composite materials consisting of polystyrene or glass spheres in ferrofluid; and,
- (iii) Composite materials consisting of non-magnetic metal particles in ferrofluid.

All categories have been examined and characterised by magnetic measurements and by optical studies. An initial preliminary study using microwaves has been undertaken using facilities at other Institutes. Some interesting features relating to an induced "dichroism" have been noticed and further study is warranted in a number of cases. It is suggested, therefore, that future work should involve

- (a) The construction of a Fourier Transform Microwave Spectrometer to enable on site measurements to be made—this has already started and some components have been acquired. The instrument should be complete within the next three months
- (b) An analysis involving microwave studies of composites containing polystyrene or glass spheres and metal particles.
- (c) A further extended study of the carrier ferrofluid.
- (d) An examination of the properties of thin films (thickness $< 100\mu\text{m}$) which appear to show anomalous behaviour.
- (c) A study of the relaxation phenomena in the materials identified in (b), (c) and (d).

The labyrinthine instability is not likely to produce any important results but the new measurements on composites look promising and more attention should be focussed on these. The carrier ferrofluids need to be studied in order that their intrinsic properties can be interpreted and used to develop new and more interesting composites. The carrier ferrofluids have been known to show an induced dichroism in the microwave region which has not yet been completely investigated and more measurements are needed. All ferrofluids show a dichroism, birefringence and Faraday rotation at optical wavelengths but the magnitude of these effects at 1-4mm wavelengths is still under investigation.

Finally, it is proposed that a theoretical study be undertaken in parallel with the experimental studies on the composites using the Monte-Carlo calculations so successfully employed in the analysis of the magnetic and optical properties of magnetic fluids. Theory which relates to a two dimensional system of equal sized spheres will be more applicable to composites containing polystyrene or glass spheres than for a three dimensional

magnetic fluid containing particles with a size distribution. Good agreements between theory and experiment is, therefore, expected.

The production of composite colloids containing non-magnetic metal particles is novel and could lead to interesting applications. It may be worth considering whether this material should be the subject of a patent application.

5.

ACKNOWLEDGEMENTS

The Authors would like to thank Dr.G.E.Evans of U.C.W., Aberystwyth, for providing Fourier Transform Spectrometer facilities, and his assistance in the measurements.

Thanks are also due to British Telecom, Ipswich, for supplying the Grubb-Parsons polarizing interferometer, for use at Bangor.

S.Wells, (U.C.N.W.,Bangor) is thanked for help in preparing ferrofluid samples and Ms.Tina Nicklin for typing this manuscript.

6.

REFERENCES

1. Davies H.W and J.P.Llewellyn (1979) J. Phys.D.12, 311-319.
2. Davies H.W and Llewellyn (1980) J.Phys.D.13, 2327-2336.
3. Mehta R.V. (1983) J.Magn. Magn. Mats 39, 64.
4. Llewellyn J.P (1983) J.Phys. D. 16, 95-104.
5. Bradbury A, S.Menear and R.W.Chantrell, Proc of Conf. on Magnetism and Magn. Mats, San Diego(1984).To be published.
6. Skjeltorp, A.T. (1983) 51 No. 25, 2306.
7. Néel L., (1947) Comptes Rend. 224, 1550.
8. Bean C.P. and J.D.Livingstone (1959) J.Appl.Phys. 30, No.4, 120.
9. Chantrell R.W., A.Bradbury, J.Popplewell and S.W.Charles, (1980) J.Phys.D.Appl.Phys. 13, L119.
10. O'Grady,K, J.Popplewell and S.W.Charles (1983), J.Magn.Magn.Mats 39, 86.
11. Menear,S., A.Bradbury and R.W.Chantrell (1983), J.Magn.Magn.Mats 39, 17.
12. Menear,S., A.Bradbury, R.W.Chantrell and K.O'Grady, (1984), Proc.of Intermag. Conf. Hamburg. To be published.
13. Tsebers,A.O and M.M.Maiorov (1980) Magnetohydrodynamics,No.2, 22.
14. Rosensweig,R.E (1983) J.Magn.Magn.Mats 39, 127.
15. Romankiw,L.T, M.M.G.Slusarczyk and D.A.Thomson (1975), IEEE Trans.on.Magn. Mag 11, No.1. 25.
16. Shimoizaka,K, Vokoyama,H., and Nakatsuka (1981), J.Jpn.Soc. Powder Metall. 28, 210.
17. Hess,P.H and Parker,P.M., (1966),J.Appl Polymer Sci. 10, 1915.
18. Charles,S.W. and J.Popplewell, (1980) IEEE Trans. Magn.Mag-16, 172.
19. Chamberlain,J. (1979), Principles of Interferometric Spectroscopy, Pub. Wiley.
20. Evans,M.E., Evans, G.J., and Davies ,R. (1976), Advances in Chemical Physics, 14 Ch.6, 242.
21. O'Grady,K. and Bradbury,A. (1983). J.Mag.Magn.Mats 39, 91.
22. Chantrell,R.W.,Popplewell,J. and Charles,S.W. (1978) IEEE Trans on Mag-12, No.6, 795.

23. Taketomi, S., (1983), Jap.J.Appl. Phys. 22, No 7, 1137.
24. Haas, W.E.L. and Adams, J.E., (1975), Appl. Phys. Letters, 27, 571.
25. Berkowitz, A.E., Lahut, J.A. and VanBuren, C.E., (1980) IEEE Trans. on Magn. Mag - 16, No.2, 184.

END

FILMED

6-85

DTIC